Australian Government
Department of Defence
Defence Science and
Technology Organisation

DSTO

Clutter Spatial Distribution and New Approaches of Parameter Estimation for Weibull and K-Distributions

Yunhan Dong

DSTO-RR-0274

Australian Government
Department of Defence
Defence Science and
Technology Organisation

Clutter Spatial Distribution and New Approaches of Parameter Estimation for Weibull and K- Distributions

Yunhan Dong

Electronic Warfare Division
Electronics and Surveillance Research Laboratory

DSTO-RR-0274

ABSTRACT

The spatial distribution of surface clutter in general depends on radar resolution, grazing angle and scatterers on the surface. The Weibull, K- and lognormal distributions are commonly used to approximate the clutter spatial distribution. Comparisons among all three distributions are reviewed and extended. Statistical properties of the Weibull and K- distributions in the log domain are derived and then used in new approaches, named as unbiased estimation schemes, for faster parameter estimation for the Weibull and K- distributions. The maximum likelihood estimates for the K-distribution are also derived without the need of the derivative of the Bessel funtion. The proposed unbiased estimation schemes provide nearly as identical estimates as the maximum likelihood scheme does, according to real aperture radar data and synthetic aperture radar data analysed.

Published by

DSTO Systems Sciences Laboratory
PO Box 1500
Edinburgh South Australia 5111

Telephone: (08) 8259 5555
Fax: (08) 8259 6567

AR-013-086
April 2004

Clutter Spatial Distribution and New Approaches of Parameter Estimation for Weibull and K- Distributions

EXECUTIVE SUMMARY

This report presents the result of a study of the clutter spatial distribution carried out under the task AIR02/232 (AEW&C SUPPORT).

Clutter return from sea and land severely limits the performance of radar surveillance systems. The motivation for determining the correct clutter spatial distribution is that the long 'tails' of the distribution are crucial for setting target detection thresholds, in order to minimise both false alarms and missed detections.

The clutter spatial distribution is complex and varies from situation to situation. It depends on not only the characteristics of random scatterers, but also radar resolution and the geometry of illumination (grazing angle), as well as radar frequency and polarisation. In the case where the radar resolution is low and the illuminated surface is homogeneous, the clutter distribution is or is close to a Rayleigh. But in the case where the radar resolution is high to very high and the grazing angle is low, the clutter distribution of even a homogeneous land or sea surface significantly diverges from a Rayleigh due to the effects of shadowing and multipath propagation. The Weibull, K- and lognormal distributions are commonly used to represent clutter spatial distributions for various situations. However, some issues related to these distributions, such as faster parameter estimation schemes deserve a research effort.

The contribution of this report is three-fold.

Comparisons among these three distributions are reviewed and extended. It is found that the difference between the Weibull and K- distributions is small when the shape parameter is within a certain range (often clutter distributions are well within this range). Previous comparisons appearing in literature are found to be incomplete.

In general, clutter distributions are often plotted on a semi-logarithm scale, i.e., clutter is expressed in decibel (dB). Statistics of distributions calculated in the log domain are desirable. The mean, standard deviation (or variance) and so forth for the Weilbull and

K- distributions in the log domain, which were previously not available, are derived. In this report these properties are later used in the parameter estimation schemes.

Parameter estimation is an important issue and the maximum likelihood (ML) estimates are the optimal. Previous research concentrated on using the Lagrange method to find the ML estimates. This seems inappropriate for the K-distribution since the derivative of the embedded Bessel function cannot be expressed in a closed form. It is therefore very difficult to find the ML estimates for the K-distribution using the Lagrange method, if not impossible. This report proposes a direct method of finding the ML estimates for the K-distribution. The direct method does not require the derivative of the Bessel function. The ML schemes often serves as a benchmark for assessing other schemes.

The ML method provides the optimal parameter estimates. Unfortunately, except for the lognormal distribution, the ML estimates for both the Weibull and K- distributions involve iterative computation manipulating sample data, which may not be practical in real-time applications. In real-time data processing, fast algorithms are desirable. This report proposes two unbiased estimation schemes for estimating parameters of the Weibull and K- distributions. The results are nearly identical to the ML estimates for various data sets analysed, but the computation should be significantly faster than that of the ML algorithms.

According to both the real aperture radar data and synthetic aperture radar data analysed, the K-distribution seems marginally better than the Weibull distribution in describing the land clutter distribution, especially at the high end of the distribution. Among the three distributions, the lognormal distribution is found to be the best fit for the distribution of low grazing angle (close to zero degrees) and high resolution (the range resolution less than 1m) sea clutter data.

Author

Yunhan Dong
Electronic Warfare and Radar Division

Dr Yunhan Dong received his Bachelor and Master degrees in 1980s in China and his PhD in 1995 at UNSW, Australia, all in electrical engineering. He then worked at UNSW from 1995 to 2000, and Optus Telecommunications Inc from 2000 to 2002. He joined DSTO as a Senior Research Scientist in 2002. His research interests are primarily in radar signal and image processing, and radar backscatter modelling. Dr Dong was a recipient of both the Postdoctal Research Fellowships and Research Fellowships from the Australian Research Council.

Contents

1. Introduction

Clutter return from sea and land severely limits the performance of radar surveillance systems. The motivation for determining the correct clutter spatial distribution is that the long 'tails' of the distribution are crucial for setting target detection threshold, in order to minimise both false alarms and missed detections.

Clutter statistics are complex, and its variations vary from situation to situation. It is well known that the fluctuations of thermal noise, or clutter return from scatterers of approximately equal magnitude randomly distributed in space, obey Rayleigh statistics. However it has been found that when measuring a complex target or clutter, the probability of relatively large signal occurrence is higher than that predicted from a Rayleigh model. Such distributions are said to have long tails. In general, if radar looks at natural land with a low resolution, the clutter distribution is or is very close to Rayleigh. However in the case of high and very high resolution radars, the resultant distribution is generally much wider. Additionally, clutter return at low grazing angles does not obey the Rayleigh distribution because of effects of shadowing and multipath propagation. Therefore, the Weibull, K- and lognormal distributions are most commonly used to describe clutter statistics (the Rayleigh distribution is a special case of the Weibull or K- distributions). Characteristics of these three distributions have been considerably studied and reported (Jao, 1984, Watts, 1985, 1987, Oliver, 1993, Blacknell, 1994, Antipov, 1998, Long, 1992, 2001, Billingsley, 2002).

The contribution of this report is three-fold.

Comparisons among these three distributions are reviewed and extended. It is found that the difference between the Weibull and K- distributions is small when the shape parameter is within a certain range (often clutter distributions are well within this range). Previous comparisons such as those given by Billingsley (2002) are found to be incomplete.

In general, clutter distributions are often plotted on a semi-logarithm scale, i.e., clutter is expressed in decibel (dB). Statistics of these distributions calculated in the log domain are desirable. The mean, standard deviation (variance) and so forth for the Weilbull and K- distributions in the log domain, which were previously not available, are derived. In this report these properties are later used in the parameter estimation schemes.

The main contribution of the report is relevant to parameter estimation for both the Weibull and K- distributions. Previous research concentrated on using the Lagrange method to find the maximum likelihood (ML) estimates. This seems inappropriate for the K-distribution since the derivative of the (imbedded) Bessel function cannot be expressed in a closed form. It is therefore very difficult to find the ML estimates for the K-distribution using the Lagrange method, if not impossible. This report proposes a

direct method to find the ML estimates for the K-distribution. The direct method does not require the derivative of the Bessel function.

Theoretically the ML estimates are the optimal. Unfortunately, iterative algorithms manipulating sample data are involved in determining the ML estimates for both the Weibull and K- distributions, which may not be practical for real-time applications. In real-time data processing fast algorithms are desirable. This report also proposes two unbiased parameter estimation schemes for the Weibull and K- distributions. The estimates are simple and yet found to be nearly identical to the ML estimates for both the real aperture radar (RAR) and synthetic aperture radar (SAR) data analysed.

2. Weibull, K- and Lognormal Distributions

2.1 Weibull Distribution

The Weibull distribution has been found to provide a good fit to both sea and land clutter (Billingsley, 2002). The probability density function (pdf) of the Weibull distribution on a linear scale is,

$$p(x) = bcx^{b-1}\exp(-cx^{b}) \qquad x > 0 \tag{1}$$

where $a = 1/b$ and c are often referred to as the Weibull shape and scale parameters, respectively.

The cumulative distribution function (cdf) of the Weibull distribution is,

$$P(x) = 1 - \exp(-cx^{b}) \tag{2}$$

Since clutter is in general expressed in decibel (dB), often we may prefer statistics of clutter distribution to be expressed on the dB scale. In this report, we use x to denote the random variable on the linear scale, $y = \ln x$ on the natural logarithm (NL) scale and $z = 10\log x$ on the dB scale. Because the relationship between y and z is only a constant scale factor, i.e., $z = \frac{10}{\ln 10}y$, any properties of either one would also apply to the other. This report uses both y and z: y for neat mathematical manipulations and z to express clutter in dB.

Knowing the pdf of a variable x and a unique function $y = y(x)$, we want to find the pdf of y. Because the interval $(x, x+dx)$ is mapped onto the interval $(y, y+dy)$, the probability of the variables falling in the intervals is the same. That is,

$$p(x)dx = p(y)dy \tag{3}$$

Because $p(y)$ has to be ≥ 0, so we have

$$p(y) = p(x)\left|\frac{dx}{dy}\right| \tag{4}$$

In the NL and dB domains, respectively, the pdfs of the Weibull distribution become,

$$p(y) = bc\left(e^{y}\right)^{b} \exp\left(-c\left(e^{y}\right)^{b}\right) \tag{5}$$

$$p(z) = \frac{1}{k_0} bc\left(10^{z/10}\right)^{b} \exp\left(-c\left(10^{z/10}\right)^{b}\right) \tag{6}$$

where $k_0 = 10/\ln 10$.

Table 1 lists statistics of the Weibull distribution. Properties on the linear scale are available in literature (e.g., Billingsley, 2002, Long 2001). Derivations of the properties in the NL and dB domains are given in Appendix A.

Table 1: Statistics of the Weibull distribution in the linear, NL and dB domains, respectively.

Property	Linear domain	NL domain	DB domain
Pdf	$p(x) = bcx^{b-1} \exp(-cx^{b})$	$p(y) = bc\left(e^{y}\right)^{b} \exp\left(-c\left(e^{y}\right)^{b}\right)$	$p(z) = \frac{1}{k_0} bc\left(10^{z/10}\right)^{b} \exp\left(-c\left(10^{z/10}\right)^{b}\right)$
Cdf	$P(x) = 1 - \exp(-cx^{b})$	$P(y) = 1 - \exp\left(-c\left(e^{y}\right)^{b}\right)$	$P(z) = 1 - \exp\left(-c\left(10^{z/10}\right)^{b}\right)$
Mean	$\frac{\Gamma(1+a)}{c^{a}}$	$-\frac{1}{b}(\gamma + \ln c)$	$-\frac{k_0}{b}(\gamma + \ln c)$
Median	$\frac{(\ln 2)^{a}}{\Gamma(1+a)}\bar{x}$	$\frac{1}{b}\left[\ln(\ln 2) - \ln c\right]$	$\frac{k_0}{b}\left[\ln(\ln 2) - \ln c\right]$
Mode	$\left(\frac{b-1}{cb}\right)^{a}$ *for* $a < 1$	$-\frac{\ln c}{b}$	$-k_0 \frac{\ln c}{b}$
Variance	$\left(\frac{\Gamma(1+2a)}{\Gamma^{2}(1+a)} - 1\right)\bar{x}^{2}$	$\frac{\pi^{2}}{6b^{2}}$	$\frac{k_0^{2}\pi^{2}}{6b^{2}}$
Std	$\left(\frac{\Gamma(1+2a)}{\Gamma^{2}(1+a)} - 1\right)^{1/2} \bar{x}$	$\frac{\pi}{\sqrt{6}b}$	$\frac{k_0\pi}{\sqrt{6}b}$

where $\gamma = -\psi^{(0)}(1) = 0.5772156649$, is Euler's Gamma constant.

2.2 K-Distribution

Many researchers have reported that both sea clutter and land clutter obey the K-distribution (Jao, 1984, Watts, 1985 and 1987, Oliver, 1993). The K- distribution has been well interpreted by Ward et al, who named it the compound K-distribution (Ward et al, 1990). The particular significance of the K-distribution is its compound nature, which interprets clutter comprising two components: a fast component (correlation time about 10ms for sea clutter at X-band), described as a Rayleigh distribution, models the local speckle; and a slow component (correlation time in the order of seconds for sea clutter at X-band), characterised by a gamma distribution, models the underlying mean of the speckle level, also referred to as texture (Gini et al, 2001, Gini and Greco, 2002). It has been found that the compound K-distribution model accurately describes real sea clutter collected by a vertically polarised X-band radar at a low grazing angle (Farina, 2002).

There are at least two versions of the K- distribution, one for square law detection (power domain) and the other for amplitude detection (voltage domain). However they are slightly different. The expression for square law detection given by Jao (1984) is,

$$p(x)=\frac{2\alpha}{\Gamma(\alpha)\bar{x}}\left(\frac{\alpha x}{\bar{x}}\right)^{\frac{\alpha-1}{2}}K_{\alpha-1}\left(2\sqrt{\frac{\alpha x}{\bar{x}}}\right)\qquad x>0 \tag{7}$$

where $K_{\upsilon}(\cdot)$ is the modified Bessel function of the second kind.

The expression for amplitude detection is (Watts 1985, 1987, Antipov 1998, Long 2001),

$$p(t)=\frac{2c}{\Gamma(\alpha)}\left(\frac{ct}{2}\right)^{\alpha}K_{\alpha-1}(ct) \tag{8}$$

By substituting $u=x^{1/2}$ and $d=2\sqrt{\alpha/\bar{x}}$ into (7), we have,

$$p(u)=\frac{2d}{\Gamma(\alpha)}\left(\frac{du}{2}\right)^{\alpha}K_{\alpha-1}(du) \tag{9}$$

On the surface, (9) appears exactly the same as (8), but they are actually not. In (8) parameters α and c are assumed to be independent while parameter d in (9) is dependent on parameter α. This difference will lead to different expressions when we manipulate the pdf with respect to parameters (parameters are treated as variables), such as $\frac{\partial}{\partial\alpha}p(x)$, in order to find the parameter estimates using the ML method, for

example. However in terms of the statistics of the distribution (parameters are treated as constants), both (7) and (8) should be the same. In this report we adopt (7) as the K-distribution, which has been widely used (Billingsley, 2002, Oliver 1993), consistent with the Weibull and lognormal distributions for the square law detection.

The pdfs of the K-distribution when the variable is expressed in the NL and dB domains, respectively, are,

$$p(y) = \frac{2}{\Gamma(\alpha)}\left(\frac{\alpha}{\bar{x}}e^{y}\right)^{\frac{\alpha+1}{2}} K_{\alpha-1}\left(2\sqrt{\frac{\alpha}{\bar{x}}e^{y}}\right) \tag{10}$$

$$p(z) = \frac{1}{k_0}\frac{2}{\Gamma(\alpha)}\left(\frac{\alpha}{\bar{x}}10^{z/10}\right)^{\frac{\alpha+1}{2}} K_{\alpha-1}\left(2\sqrt{\frac{\alpha}{\bar{x}}10^{z/10}}\right) \tag{11}$$

The statistics of the K-distribution in the linear, NL and dB domains, respectively, are given in Table 2. The corresponding derivations can be found in Appendix A.

Table 2: Statistics of K-distribution in the linear, NL and dB domains, respectively.

Property	Linear domain	NL domain	DB domain
Pdf	$p(x) = \frac{2\alpha}{\Gamma(\alpha)\bar{x}}\left(\frac{\alpha x}{\bar{x}}\right)^{\frac{\alpha-1}{2}} K_{\alpha-1}\left(2\sqrt{\frac{\alpha x}{\bar{x}}}\right)$	$p(y) = \frac{2}{\Gamma(\alpha)}\left(\frac{\alpha}{\bar{x}}e^{y}\right)^{\frac{\alpha+1}{2}} \cdot K_{\alpha-1}\left(2\sqrt{\frac{\alpha}{\bar{x}}e^{y}}\right)$	$p(z) = \frac{1}{k_0}\frac{2}{\Gamma(\alpha)}\left(\frac{\alpha}{\bar{x}}10^{z/10}\right)^{\frac{\alpha+1}{2}} \cdot K_{\alpha-1}\left(2\sqrt{\frac{\alpha}{\bar{x}}10^{z/10}}\right)$
Cdf	$P(x) = 1-\frac{2}{\Gamma(\alpha)}\left(\frac{\alpha x}{\bar{x}}\right)^{\alpha/2} K_{\alpha}\left(2\sqrt{\frac{\alpha x}{\bar{x}}}\right)$	$P(y) = 1-\frac{2}{\Gamma(\alpha)}\left(\frac{\alpha e^{y}}{\bar{x}}\right)^{\alpha/2} K_{\alpha}\left(2\sqrt{\frac{\alpha e^{y}}{\bar{x}}}\right)$	$P(z) = 1-\frac{2}{\Gamma(\alpha)}\left(\frac{\alpha 10^{y/10}}{\bar{x}}\right)^{\alpha/2} K_{\alpha}\left(2\sqrt{\frac{\alpha 10^{y/10}}{\bar{x}}}\right)$
Mean	$\bar{x}$	$-\gamma+\psi^{(0)}(\alpha)-\ln\frac{\alpha}{\bar{x}}$	$k_0\left(-\gamma+\psi^{(0)}(\alpha)-\ln\frac{\alpha}{\bar{x}}\right)$
Variance	$\left(1+\frac{2}{\alpha}\right)\bar{x}^2$	$\psi^{(1)}(\alpha)+\frac{\pi^2}{6}$	$k_0{}^2\left(\psi^{(1)}(\alpha)+\frac{\pi^2}{6}\right)$
Std	$\left(1+\frac{2}{\alpha}\right)^{1/2}\bar{x}$	$\left(\psi^{(1)}(\alpha)+\frac{\pi^2}{6}\right)^{1/2}$	$k_0\left(\psi^{(1)}(\alpha)+\frac{\pi^2}{6}\right)^{1/2}$

Where $\psi^{(n)}(x)$ is the Polygamma function, defined as the n^{th} derivative of the logarithm of the Gamma function, $\frac{d^{n+1}}{dx^{n+1}}(\ln\Gamma(x))$.

It can be proven that a Weibull distribution with $b=1$ is equivalent to a K-distribution with $\alpha=\infty$, and both distributions are identical to the negative exponential distribution, i.e., the Rayleigh distribution, as (Jao, 1984),

$$p(x)=\frac{1}{\bar{x}}\exp\left(-x/\bar{x}\right) \tag{12}$$

A Weibull distribution with $b=1/2$ is again identical to a K-distribution with $\alpha=1/2$ (Davidson, et al, 2002). This can be easily proven if we note (Gradshteyn and Ryzhik, 1980),

$$K_{-1/2}(x)=\sqrt{\frac{\pi}{2x}}\exp(-x) \tag{13}$$

2.3 Lognormal distribution

The distribution of a random variable x is lognormal, if $\ln x$ is normally distributed with mean μ and variance s^2. The pdf of the lognormal distribution is given by,

$$p(x)=\frac{1}{\sqrt{2\pi}s}\frac{1}{x}\exp\left(-\frac{1}{2s^2}(\ln x-\mu)^2\right) \qquad x>0 \tag{14}$$

The cdf of the lognormal distribution is

$$P(x)=\frac{1}{2}\left[1+sign(u)erf(|u|)\right] \tag{15}$$

where $u=\frac{\ln x-\mu}{\sqrt{2}s}$; $sign(\cdot)$ is the sign function; and $erf(\cdot)$ is the error function, defined as

$$erf(u)=\frac{2}{\sqrt{\pi}}\int_0^u\exp(-t^2)dt \qquad u\geq 0 \tag{16}$$

The pdfs of the lognormal distribution when the variable is expressed in the NL and dB domains, respectively, are,

$$p(y)=\frac{1}{\sqrt{2\pi}s}\exp\left(-\frac{1}{2s^2}(y-\mu)^2\right) \tag{17}$$

$$p(z)=\frac{1}{k_0}\frac{1}{\sqrt{2\pi}s}\exp\left(-\frac{1}{2s^2}(\frac{z}{k_0}-\mu)^2\right) \tag{18}$$

Compared to the Weibull and K- distributions, the convergence of the cdf of the lognormal distribution is the slowest, i.e., its 'tail' is longest. Therefore, the lognormal distribution has been used extensively in cases where echo/clutter fluctuations attain large values for much higher percentages than Weibull and K-distribution statistics (Long, 2001).

Table 3 lists statistics of the lognormal distribution in the linear, NL and dB domains, respectively.

Table 3: Statistics of the lognormal distribution in the linear, NL and dB domains, respectively.

Property	Linear domain	NL domain	DB domain
Pdf	$p(x)=\frac{1}{\sqrt{2\pi}s}\frac{1}{x}$ $\exp\left(-\frac{1}{2s^2}(\ln x-\mu)^2\right)$	$p(y)=\frac{1}{\sqrt{2\pi}s}$ $\exp\left(-\frac{1}{2s^2}(y-\mu)^2\right)$	$p(z)=\frac{1}{k_0}\frac{1}{\sqrt{2\pi}s}$ $\exp\left(-\frac{1}{2s^2}(\frac{z}{k_0}-\mu)^2\right)$
Cdf	$P(x)=\frac{1}{2}[1+sign(u)erf(\vert u\vert)]$ where $u=\frac{\ln x-\mu}{\sqrt{2}s}$	$P(y)=\frac{1}{2}[1+sign(u)erf(\vert u\vert)]$ where $u=\frac{y-\mu}{\sqrt{2}s}$	$P(z)=\frac{1}{2}[1+sign(u)erf(\vert u\vert)]$ where $u=\frac{z/k_0-\mu}{\sqrt{2}s}$
Mean	$\exp(\mu+s^2/2)$	μ	$k_0\mu$
Median	$\exp(\mu)$	μ	$k_0\mu$
Mode	$\exp(\mu-s^2)$	μ	$k_0\mu$
Variance	$[\exp(s^2)-1]\bar{x}^2$	s^2	$k_0{}^2s^2$
Std	$[\exp(s^2)-1]^{1/2}\bar{x}$	s	k_0s

3. Comparisons Among Weibull, K- and Lognormal Distributions

Because the logarithmic transform is non-linear with low values being stretched and high values compressed, the same distribution on the linear scale and the dB scale might look significantly different. As clutter is generally expressed in dB, we mainly concentrate our discussion of distributions on the dB scale.

3.1 Same Mean and Same Standard Deviation in the Linear Domain

We assume $\bar{x}=1$, as it is only a matter of scaling in the linear domain or a matter of shift in the dB domain if the actual mean value is different. We also assume $std(x)$ (standard deviation of x) is the same for all three distributions in each case for the purpose of comparison. In particular, Table 4 shows mean and std values when calculated in the dB domain for four cases, corresponding to $a=1,1.5,2,3$ for the Weibull distribution, respectively. A Weibull distribution with $a=1$ is the same as a K-

distribution with $\alpha = \infty$, and both simplify to the Rayleigh distribution. A Weibull distribution with $a = 2$ is also the same as a K-distribution with $\alpha = 0.5$. Although in each case, $E(x)$ and $std(x)$ are the same for all three distributions, $E(z)$ and $std(z)$ for the three distributions diverse remarkably especially when $std(x)$ becomes larger.

Table 4: Distribution comparison from the perspective on the mean and std in the dB domain giving the mean and std in the linear domain to be the same for all three distributions.

	Weibull	K-	Lognormal
	Case 1: $E(x)=1$; $a=1$ ($std(x)=1$)		
Parameters	$a=1$; $c=1$	$\alpha=\infty$	$\mu=-0.3466$; $s=0.8326$
$E(z)$	-2.5dB	-2.5dB	-1.5dB
$std(z)$	5.6dB	5.6dB	3.6dB
	Case 2: $E(x)=1$; $a=1.5$ ($std(x)=1.5477$)		
Parameters	$a=1.5$; $c=1.209$	$\alpha=1.4334$	$\mu=-0.6112$; $s=1.1056$
$E(z)$	-5.0dB	-4.2dB	-2.7dB
$std(z)$	8.4dB	7.1dB	4.8dB
	Case 3: $E(x)=1$; $a=2$ ($std(x)=2.2361$)		
Parameters	$a=2$; $c=1.414$	$\alpha=0.5$	$\mu=-0.8959$; $s=1.3386$
$E(z)$	-8.0dB	-8.0dB	-3.9dB
$std(z)$	11.1dB	11.1dB	5.8dB
	Case 4: $E(x)=1$; $a=3$ ($std(x)=2.2361$)		
Parameters	$a=3$; $c=1.8171$	$\alpha=0.1111$	$\mu=-1.4979$; $s=1.7308$
$E(z)$	-15.3dB	-33.8dB	-6.5dB
$std(z)$	16.7dB	39.8dB	7.5dB

When $1 < a < 2$, the Weibull and the K- distributions are different, but the difference is small. This will become clear when we look at their pdfs and cdfs shortly. In this range, $std(z)$ of the K-distribution is less than the value of the Weibull distribution, i.e., the shape of the K-distribution is slightly narrower than the shape of the Weibull distribution. However in the range of $a > 2$, the shape of the K-distribution becomes broader than the shape of the Weibull distribution. The shape of the lognormal distribution is always the narrowest.

Figure 1 shows pdfs of Case 1, 2, and 3, respectively. In order to see the details of the distributions at the low probability ends, pdfs on the log scale are also show in the figures. It is easy to shown that the pdf of the lognormal distribution, when expressed on the log scale, becomes a quadratic function, the shape of the pdf is therefore a face down parabola symmetrical to the vertical line of $z = E(z)$. The pdf shapes of both Weibull and K- distributions are also similar to parabolas (but are not parabolas), and their quasi-symmetric axes are not vertical but tilted some degrees, leading to smaller pdf values at the high end. The 'tail' of the Weibull and the k- distributions are therefore not as long as the 'tail' of the lognormal distribution.

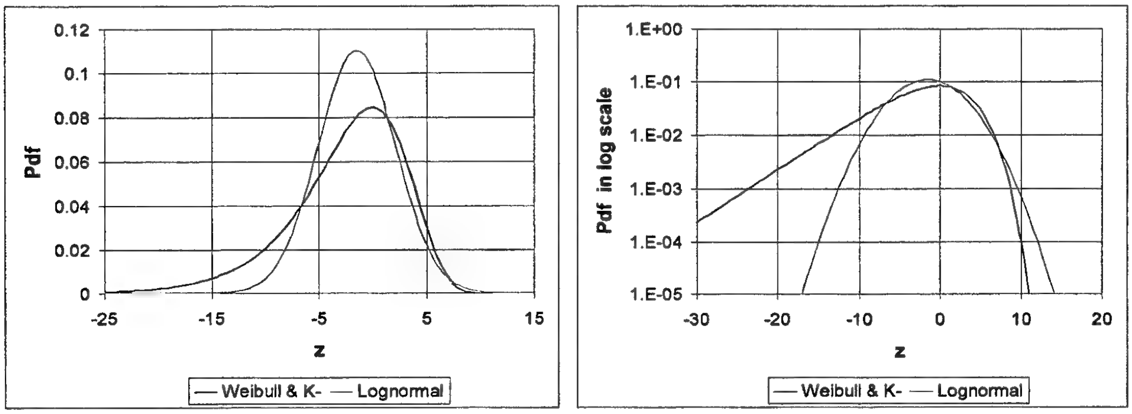

(a)

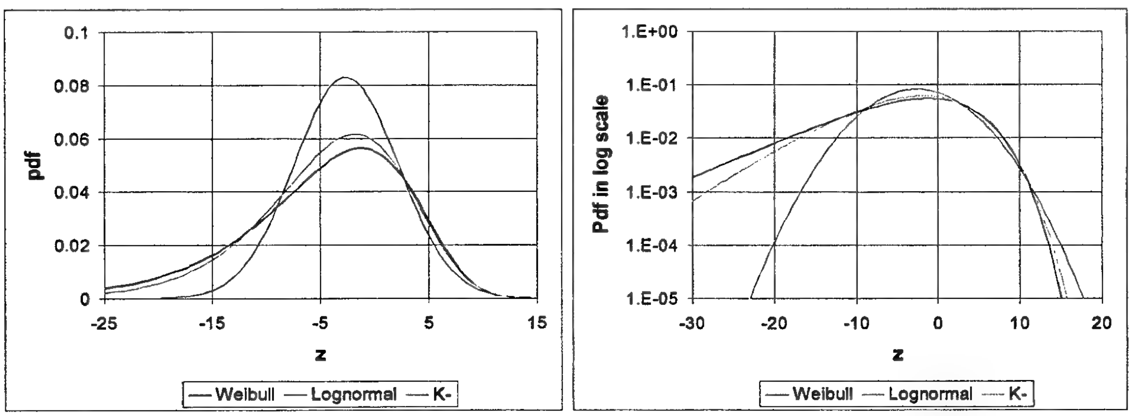

(b)

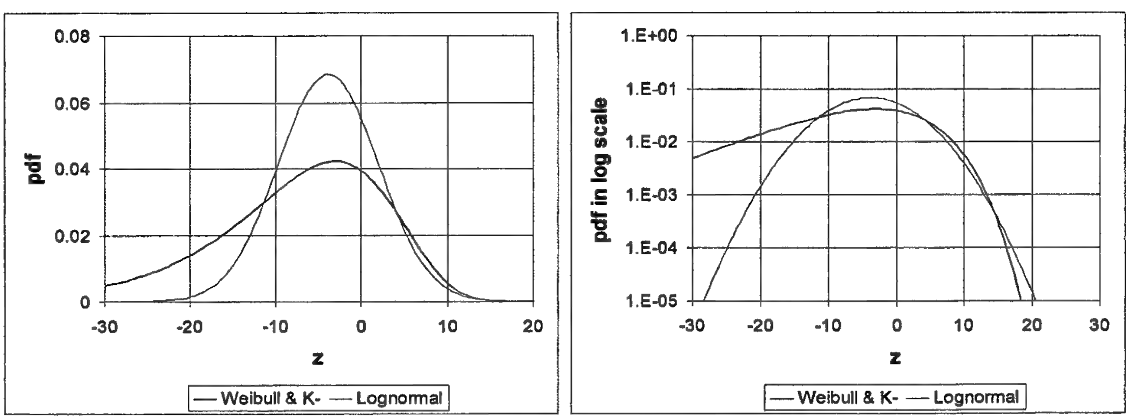

(c)

Figure 1: Comparisons of pdfs of Weibull, K- and lognormal: (a) $a=1$, (b) $a=1.5$ and (c) $a=2$ respectively. Pdfs on the log scale show details of distribution in the low probability ends.

To compare the convergence of cdf, we may plot cdfs onto the Weibull scale (Billingsley, 2002). The Weibull scale maps the cdf $P(z)$ into $10\log\left(\ln\frac{1}{1-P(z)}\right)$, so the cdf of the Weibull distribution becomes a straight line with a slope of b. Figure 2 shows cdf comparisons among the three distributions. It was reported that among the distributions, the K- distribution converges fastest, (curving up), the Weibull in the middle (straight line) and the lognormal, the slowest (curving down) (Billingsley, 2002). From Figure 2 we can see that this conclusion is incomplete. In fact only when $a>2$, is the conclusion correct, while in the range of $1<a<2$ the cdf of the K-distribution also curves down on the Weibull scale. Therefore in the $1<a<2$ range, the fastest convergence is the Weibull, followed by the K- and then the lognormal. As mentioned before, when $a=$ 1 or 2, the Weibull and the K- distributions are identical.

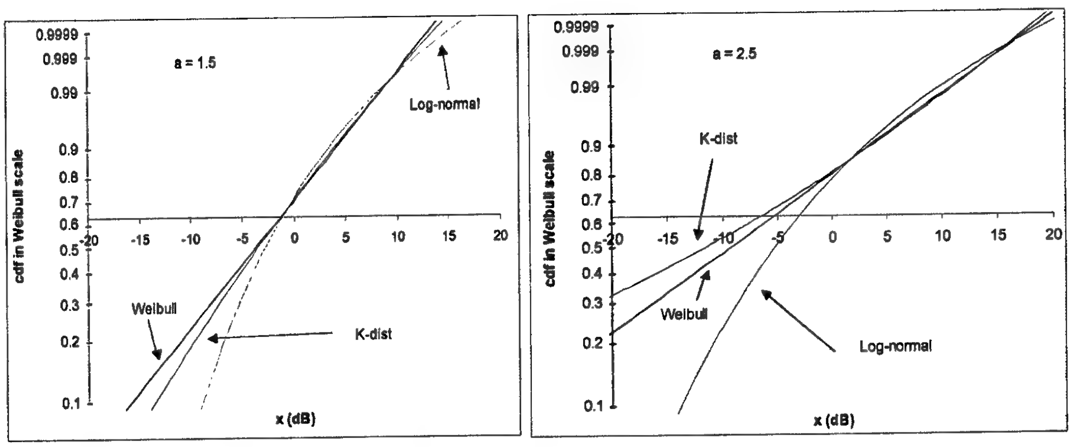

Figure 2: cdf comparisons using the Weibull scale. The cases $a=1.5$ and $a=2.5$ are shown, in which the cdf of the K-distribution curves down and up, respectively, indicating that the convergence of the K-distribution can be slower or faster than that of the Weibull distribution depending on the corresponding shape parameter.

Another way to compare the cdfs is to plot $\log(1-P(z))$, so the details of the convergence of the cdf can be viewed clearly (It is understood that if we swap the axes, then the plot will become the so called quantile distribution). Figure 3 compares the convergence of the three cdfs with $a=1.5$ and $a=2.5$, respectively. The lognormal distribution converges slowest, and requires a few dB more than the others in order to achieve the same cdf value of 0.9999.

In practice, the clutter distribution in most cases falls in the range $1<a<2$, where we have seen the differences between the Weibull and k- distributions are very small.

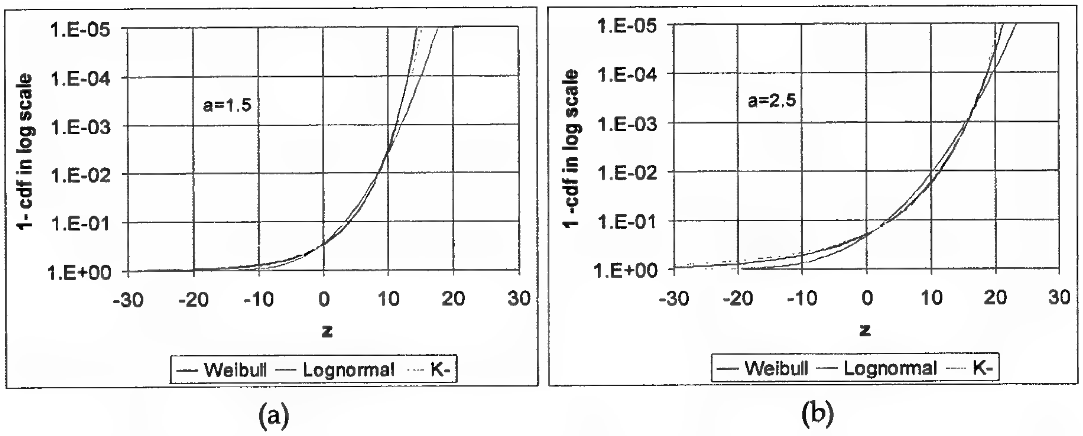

Figure 3: Cdf comparison. The term of $1-P(z)$ *is plotted on the log scale to shown the details of the convergence of the curves.*

3.2 Same Median and Same Standard Deviation in dB Domain

It can be seen in Table 4 that for the same $std(x)$ in the linear domain, the lognormal distribution usually has the smallest $std(z)$ in the dB domain. If the same std value is given in the dB domain, we can imagine that the lognormal distribution has even broader shape. The convergence of its cdf is then even slower, i.e., its 'tail' is even longer.

For illustration purposes, Figure 4 shows pdfs in which we assume the median value in the dB domain to be 0dB, and the std to be 5.6dB (corresponding to $a=1$ for the Weibull distribution) and 11.1dB (corresponding to $a=2$ for the Weibull distribution), respectively. Compared to Figure 1, where the same mean and the same std in the linear domain is assumed, the difference between the lognormal distributions and the other two widens. As shown in Figure 5, for the lognormal distribution the value of z has to be more than 10dB and 20dB higher than that of the Weibull and K-distributions, respectively, to achieve the same cdf value of 0.9999. This demonstrates the importance of the clutter distribution studies.

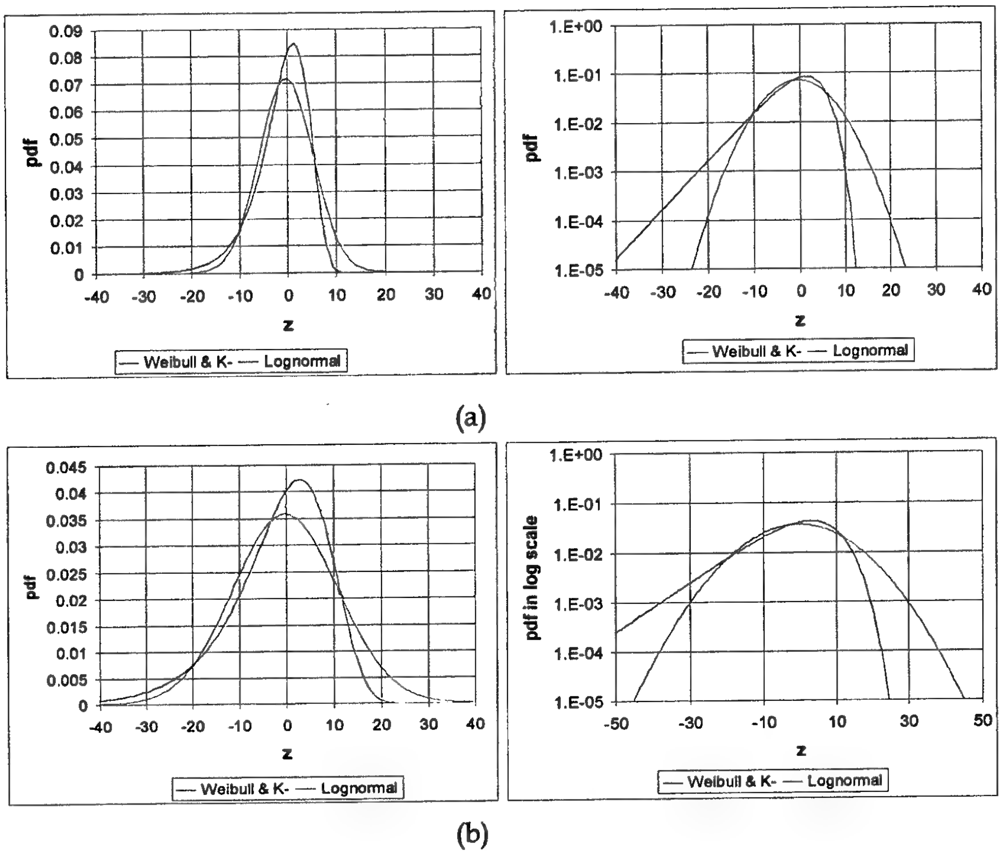

Figure 4: Comparisons of pdfs of the Weibull, K- and lognormal with the same median of 0dB, and the same std of (a) 5.6dB (equivalent to $a=1$ in the Weibull distribution) and (b) 11.1dB (equivalent to $a=2$ in the Weibull distribution) in the dB domain.

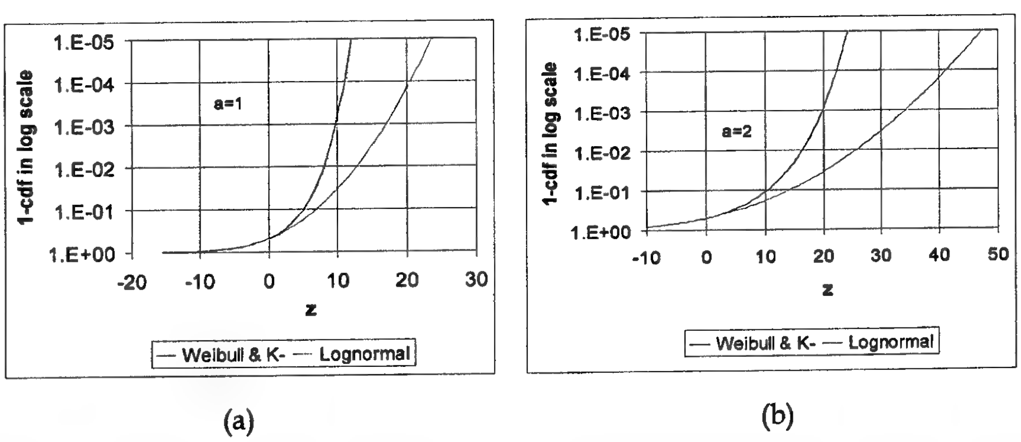

Figure 5: Comparisons of cdfs of the Weibull, K- and lognormal with the same median of 0dB and the same std of (a) 5.6dB (equivalent to $a=1$ in the Weibull distribution) and (b) 11.1dB (equivalent to $a=2$ in the Weibull distribution) in the dB domain.

4. Parameter Estimation

An important issue in the clutter distribution studies is parameter estimation. For a given pdf, its parameters determine all the corresponding statistics.

4.1 Maximum Likelihood Method

A standard approach to determining parameters is the ML method, which provides optimal parameter estimates in the sense that these estimates are the most probable parameters for the given data and the pdf, if there is no prior knowledge (Oliver, 1993, Antipov, 1998).

If n samples, $x_1, x_2, \cdots, x_n$ are given to estimate m parameters $\theta_1, \theta_2, \cdots, \theta_m$ of a given distribution function, then the joint pdf of $x_1, x_2, \cdots, x_n$ is the product of the marginal pdfs:

$$f(x_1, x_2, \cdots, x_n; \theta_1, \theta_2, \cdots, \theta_m) = \prod_{i=1}^{n} f(x_i; \theta_1, \theta_2, \cdots, \theta_m) \tag{19}$$

The estimates $\hat{\theta}_1, \hat{\theta}_2, \cdots, \hat{\theta}_m$ which maximise the joint pdf (19) are referred to as the ML estimates. In general, the estimates $\hat{\theta}_1, \hat{\theta}_2, \cdots, \hat{\theta}_m$ can be found using the Lagrange method.

Since the logarithm function is monotonic, and it transfers a product into a summation, the ML estimates can be obtained by,

$$\begin{cases} \dfrac{\partial}{\partial \theta_1} \sum_{i=1}^{n} \ln f(x_i; \theta_1, \theta_2, \cdots, \theta_m) = 0 \\ \dfrac{\partial}{\partial \theta_2} \sum_{i=1}^{n} \ln f(x_i; \theta_1, \theta_2, \cdots, \theta_m) = 0 \\ \qquad \vdots \\ \dfrac{\partial}{\partial \theta_m} \sum_{i=1}^{n} \ln f(x_i; \theta_1, \theta_2, \cdots, \theta_m) = 0 \end{cases} \tag{20}$$

4.1.1 ML Estimates of Lognormal Distribution

Using (20) it is straightforward to derive the ML estimates for the lognormal distribution:

$$\begin{cases} \hat{\mu} = \frac{1}{n}\sum_{i=1}^{n} \ln x_i \\ \hat{s}^2 = \frac{1}{n}\sum_{i=1}^{n} (\ln x_i - \hat{\mu})^2 \end{cases} \tag{21}$$

These results in fact are the mean and the variance of the samples calculated in the NL domain:

$$\begin{cases} \hat{\mu} = \langle y \rangle = E(y) \\ \hat{s}^2 = \langle y^2 \rangle - \langle y \rangle^2 = \mathrm{var}(y) \end{cases} \tag{22}$$

where $\langle \cdot \rangle$ denotes the ensemble average.

4.1.2 ML Estimates of Weibull Distribution

Appling (20) to the Weibull distribution, it is not difficult to derive the following ML estimates for the Weibull distribution (Oliver, 1993):

$$\begin{cases} \frac{1}{\hat{c}} = \frac{1}{n}\sum (x_i)^{\hat{b}} \\ \frac{1}{\hat{b}} = \frac{1}{n}\left[\hat{c}\sum_{i=1}^{n} (x_i)^{\hat{b}} \ln x_i - \sum_{i=1}^{n} \ln x_i \right] \end{cases} \tag{23}$$

Equation (23) in general cannot be solved directly, and requires an iterative solution. The iteration can be written as,

$$\begin{cases} \frac{1}{\hat{c}_k} = E\left(x^{\hat{b}_{k-1}} \right) \\ \frac{1}{\hat{b}_k} = \hat{c}_k E\left(x^{\hat{b}_{k-1}} y \right) - E(y) \end{cases} \quad k = 1, 2, \cdots \tag{24}$$

Without losing generality, we can let $\hat{b}_0 = 1$.

4.1.3 ML Estimation for K- Distribution

Given the fact that the derivative with respect to α of the modified Bessel function of the second kind is not in a closed form (in our case, α is not only the part of the variable but also the order of the function making the derivative even more complex), the ML estimates of the K-distribution, even in an iterative form, are difficult to find using (20), if not impossible. Using the Mellin transform, Oliver (1993) has derived an asymptotic expression for the K- distribution, in which the K-distribution is expressed as a Gamma distribution with a modification factor. The corresponding approximate ML estimates for the asymptotic expression have then been derived. However, the

resultant ML estimates is only applicable to the limit of large look number of multi-look data (e.g., radar measurements are averaged in the power domain, such as the multi-look SAR data). Therefore the formulae do not suit for the parameter estimation for (7) in which the look number is assumed to be one. Joughin et al (1993) have proposed a direct approach to find the ML estimates for the K- distribution. The method expresses the K-distribution as a combination of gamma and Rayleigh distributions to simplify the calculation, but the estimates have to be numerically searched.

In fact, if the calculation is not required in real-time, we can apply an iterative algorithm searching the optimal $\hat{a}$ which maximises the log-likelihood function (i.e., using (19) to search the maximum of the function rather than using (20) to search the derivative of the function to be equal to zero), because the direct search does not require the derivates of the Bessel function. Luckily, such a direct ML estimates search for the K-distribution function only requires a one-dimensional search. The parameter $\bar{x}$ does not need the optimal search, as the ML estimation of $\bar{x}$ is $E(x)$. The direct ML estimates search scheme for the K- distribution can be written as (omitting constant terms),

$$\begin{cases} \bar{x} = \frac{1}{n}\sum_{i=1}^{n} x_i = E(x) \\ \hat{\alpha} \Leftarrow \max\limits_{\alpha}\left\{ n\ln\alpha - n\ln\Gamma(\alpha) + \frac{\alpha-1}{2}\left(n\ln\alpha - n\ln\bar{x} + \sum_{i=1}^{n}\ln x_i \right) + \sum_{i=1}^{n}\ln K_{\alpha-1}\left(2\sqrt{\frac{\alpha}{\bar{x}}x_i} \right) \right\} \end{cases} \tag{25}$$

4.2 Unbiased Estimates

Theoretically the ML method provides the optimal parameters which are the most probable parameters for a given distribution and sample data. In the asymptotic limit, the ML estimates produce the smallest errors that may be calculated via the Cramer-Rao lower bound (Blacknell, 1994). Unfortunately except for the lognormal distribution, for which the ML estimates can be directly calculated via the calculation of the mean and variance (i.e., the first and second moment of the data) in the log domain, the ML estimates for both the Weibull and K- distribution involve iterative equations manipulating data samples.

Since the ML estimates are readily available for the lognormal distribution, our discussion focuses on the Weibull and K- distributions.

A few estimation methods have been suggested and investigated. Blacknell (1994) has compared three estimation schemes based on the moment method for K-distributions proposed by other researchers. Oliver (1993) has used the Mellin transform to form an iterative solution to achieve the approximate ML estimates. Menon (1963) has also suggested a way to obtain estimates for the Weibull distribution. In this report we propose two estimation schemes named as no-bias (NB) I and II estimates. The NB-I

estimation scheme estimates parameters with no bias to the mean and to the variance in the log domain ($E(z)$ and $\mathrm{var}(z)$), whereas the NB-II estimation scheme estimates parameters with no bias to the means in the linear domain as well as in the log domain ($E(x)$ and $E(z)$).

4.3 NB-I Scheme

In general, for a perfect two-parameter distribution, its parameters totally determine the mean and the variance and vice versa. Intuitively, as we are interested in the mean and the variance of a distribution, estimates providing no-bias estimation for the mean and the variance, would therefore be at least a close estimation, if not the optimum. Since the logarithmic transform is non-linear, and often we are interested in the distribution presented in the log domain, the NB-I scheme simply uses the first moment $E(z)$ and the second moment $E(z^2)$ to estimate parameters. Therefore, the scheme is no-bias estimation to the mean and variance in the log domain. In fact, we have seen that the NB-I estimates are also the ML estimates for the lognormal distribution.

4.3.1 NB-I Estimates of Weibull Distribution

Using expressions of $E(z)$ and $\mathrm{var}(z)$ shown in Table 1, the NB-I estimates for the Weibull distribution are,

$$\begin{cases} \hat{c} = \exp\left(-\gamma - \dfrac{\pi}{\sqrt{6}} \dfrac{E(z)}{std(z)}\right) \\ \hat{b} = k_0 \dfrac{\pi}{\sqrt{6}} \dfrac{1}{std(z)} \end{cases} \tag{26}$$

It can be proven that the result of (26) is the same as the result given by Menon (1963) though the derivation is different. The physical meaning of (26) is now clarified, that is, the mean and the variance in the dB domain of the Weibull distribution with parameters $\hat{b}$ and $\hat{c}$ are equal to the data's mean $E(z)$ and variance $\mathrm{var}(z)$, respectively.

There are no NB-I estimates for the K-distribution.

4.4 NB-II Scheme

In statistics when the moment method is used for parameter estimation, in general the higher the order of the moment, the bigger the error in the estimates. The NB-I scheme uses the first and the second moments to derive the estimates. Can we use the first moment only to determine the estimates? The answer is yes. In order to estimate two parameters, we may use $E(x)$ and $E(z)$. Since the transform $z = 10\log x$ is non-linear,

$E(x)$ and $E(z)$ are linearly independent though both of them are the first moment of the data. In fact $E(x)$ is the arithmetic mean and $E(z)$ the geometric mean (see Appendix A for details).

4.4.1 NB-II estimates of Weibull Distribution

Using the expressions of $E(x)$ and $E(z)$ shown in Table 1, the NB-II estimates for the Weibull distribution are,

$$\begin{cases} \ln\Gamma(1+\hat{a})+\dfrac{E(z)}{k_0}+\hat{a}\gamma-\ln E(x)=0 \\ \hat{c}=\exp\left(-\dfrac{E(z)}{k_0\hat{a}}-\gamma\right) \end{cases} \tag{27}$$

In order to numerically find $\hat{a}$ which is embedded in a non-linear equation, iteration might be required. But this iteration is different from the iteration involved in the ML method. This iteration does not need the involvement of the sample data once $E(x)$ and $E(z)$ are ready. Therefore the scheme would be much more faster than the scheme in which the sample data are involved in the iteration.

4.4.2 NB-II Estimates of K- Distribution

For the K- distribution, obviously the best estimation of $\bar{x}$ is $E(x)$, and the estimation of the α can be found from the expression for $E(z)$ shown in Table 2. The NB-II estimates for the K- distribution are,

$$\begin{cases} \bar{x}=E(x) \\ \psi^{(0)}(\hat{\alpha})-\ln\hat{\alpha}=\gamma-\ln\bar{x}+\dfrac{1}{k_0}E(z) \end{cases} \tag{28}$$

Similarly parameter $\hat{\alpha}$ can be numerically determined by solving the non-linear equation shown in (28), which is again much faster than solving the non-linear equation shown in (25) for the ML estimates where the manipulation of the sample data is involved in the iteration.

The NB-II scheme for the K- distribution is not new, and a similar scheme has been studied and reported by Raghavan (1991) and later examined by Blacknell (1994), though the derivation is different. After compared three non-ML estimate schemes, Blacknell (1994) concluded that the NB-II (though Blacknell did not use such a name for the scheme as its derivation was different then) was the best.

5. Comparisons

In this section we compare different estimation schemes using both the RAR and SAR data.

5.1 Low Resolution RAR Data of Homogenous Clutter

Data collected by the multi-channel airborne radar measurement (MCARM) system, in particular the data of the sum analogue channel, extracted from Flight 5, Circle d, Acquisition 575, are used for this case study. The data are of L-band VV low resolution (the ground patch size is about $8\times10^5 m^2$) and represent the clutter of statistically homogenous farmland. The total sample number is 762, which seems to be small for the distribution analysis, but this is the maximum number we can extract from the data set. The data need pre-processing, and the details are given in Appendix B. Since the processing gains in various stages are unknown, the mean of the samples is normalised to 1 (0dB).

The estimates calculated from the ML, NB-I and NB-II estimation schemes for the Weibull and K- distributions, respectively, are given in Table 5. To evaluate the accuracy of the NB-I and NB-II estimation schemes, we can use the ML estimates as the benchmark, as the ML estimates are optimal. According to the estimated parameters, the distribution is very close to the Rayleigh distribution, which means the corresponding parameter α of the K-distribution should approach infinity. The values of α calculated by the ML and NB-II schemes, respectively, seem to be significantly different, but it is merely the calculations converging to different points. For numerical calculation, all $\alpha \geq 25$ can be regarded as the same as $\alpha \to \infty$, this will become clear when we look at the distribution curves.

Table 5: ML NB-I and NB-II estimates of the MCARM RAR (L band VV polarisation) clutter data of farmland.

Distribution	ML estimates	No-bias estimates	
		Scheme I	Scheme II
Weibull	$\hat{a} = 0.9916$ $\hat{c} = 0.9963$	$\hat{a} = 0.9359$ $\hat{c} = 1.0118$	$\hat{a} = 0.9738$ $\hat{c} = 0.9889$
K-	$\bar{x} = 1.000$ $\hat{\alpha} = 25.5876$	N/A	$\bar{x} = 1.0000$ $\hat{\alpha} = 72.0000$

The pdfs and cdfs of the Weibull distribution using the ML, NB-I and NB-II estimates are plotted in Figure 6, while the pdfs and cdfs of the K-distribution using the ML and NB-II estimates are plotted in Figure 7. In order to examine the details of the distribution at the ends, the pdfs on the log scale are also plotted. The cdfs are also plotted on the log scale, since we are more interested in the high end.

It can be seen that the difference between the ML estimates and the NB-II estimates for both the Weibull and the K- distributions, respectively, is insignificant, and the corresponding pdfs and cdfs are nearly identical. The NB-I estimates are also good, but not as good as the NB-II estimates.

The comparison between the Weibull and the K- distributions are shown in Figure 8. The K- distribution converges a little bit slower. If we view Figure 6 and Figure 7 carefully, the K-distribution seems a little better to represent the data distribution especially at the higher end.

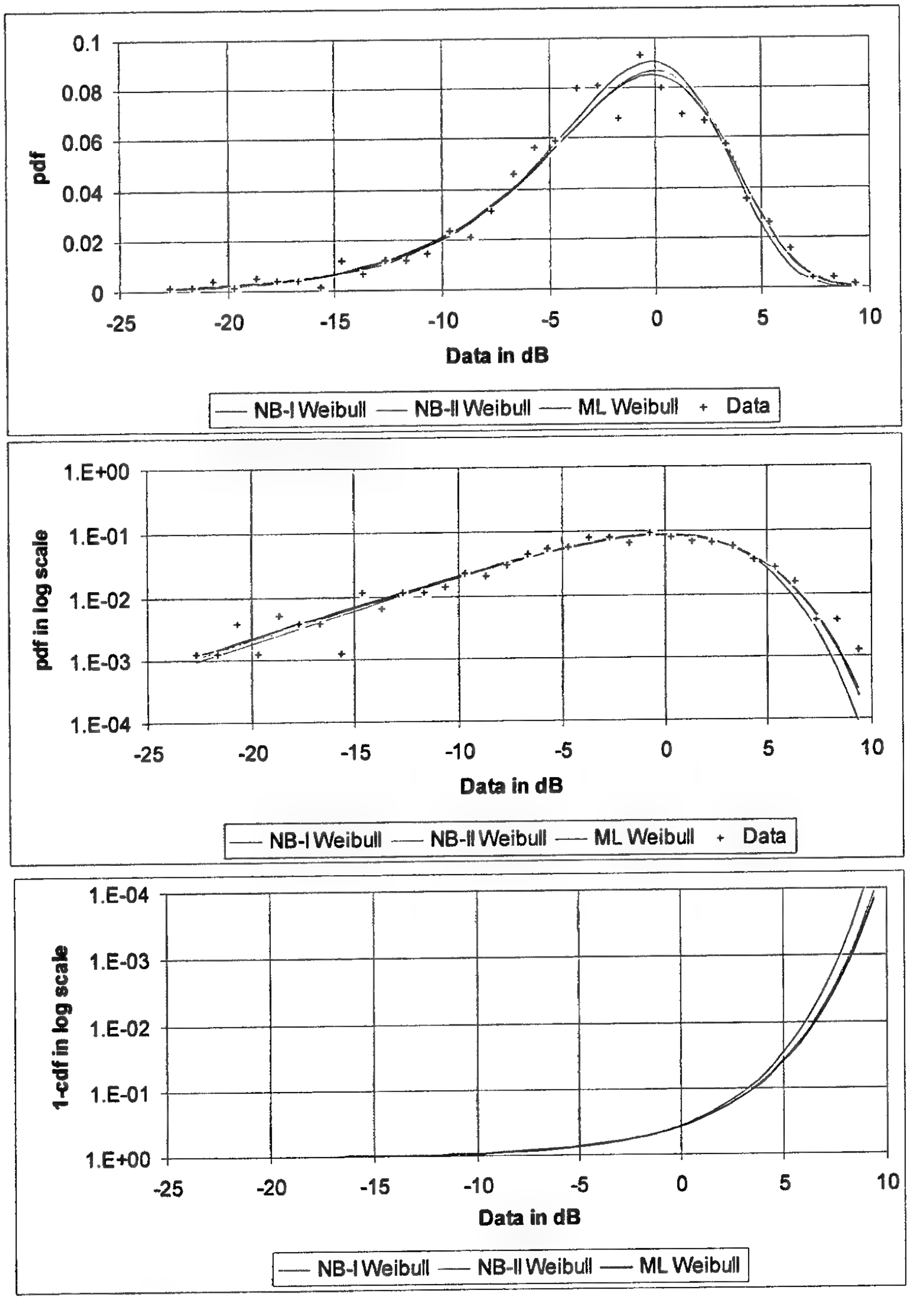

Figure 6: Comparison of parameter estimation schemes for the Weibull distribution using the MCARM RAR L-band VV clutter data of homogenous farmland.

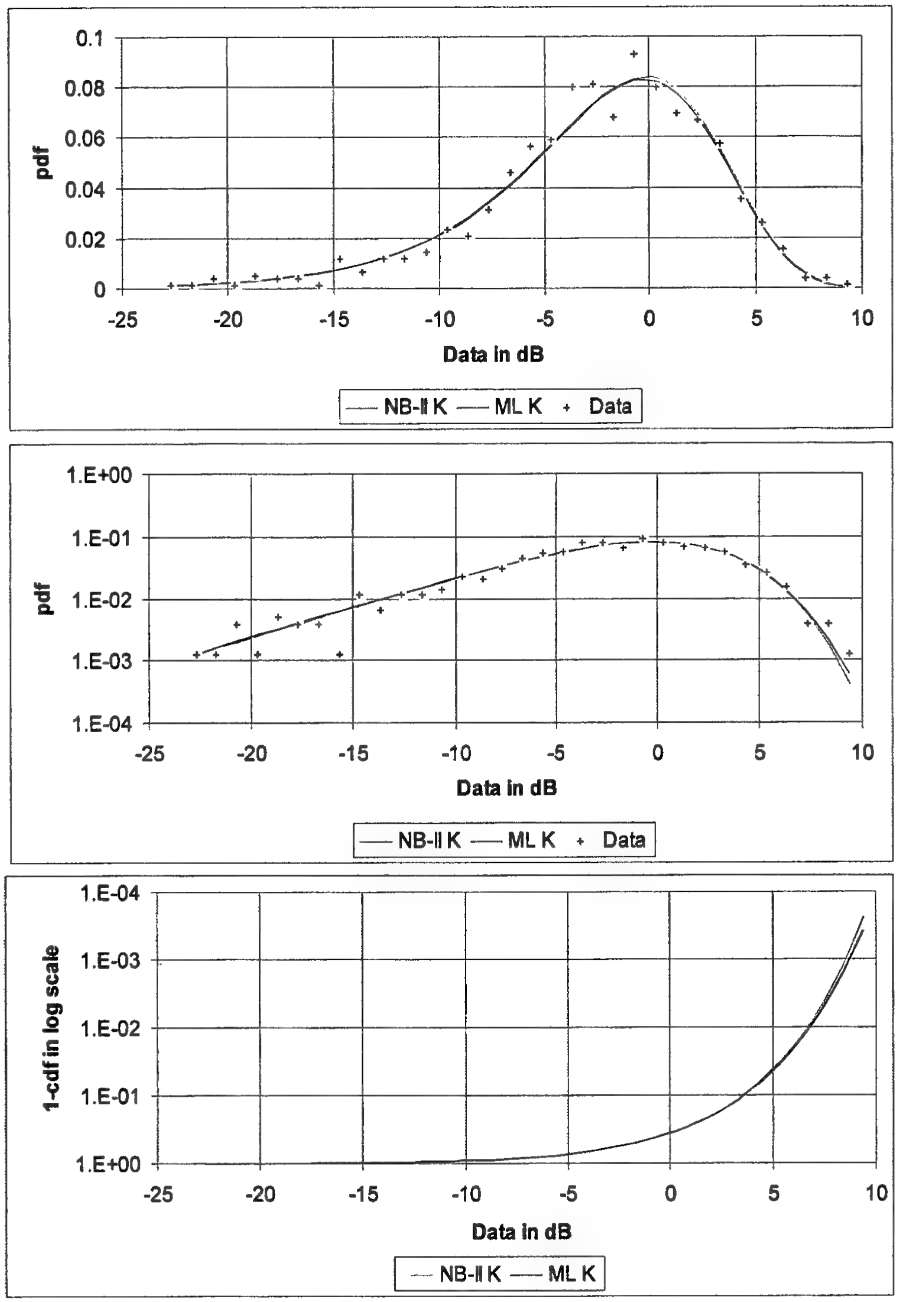

Figure 7: Comparison of parameter estimation schemes for the K-distribution using the MCARM RAR L-band VV clutter data of homogeneous farmland.

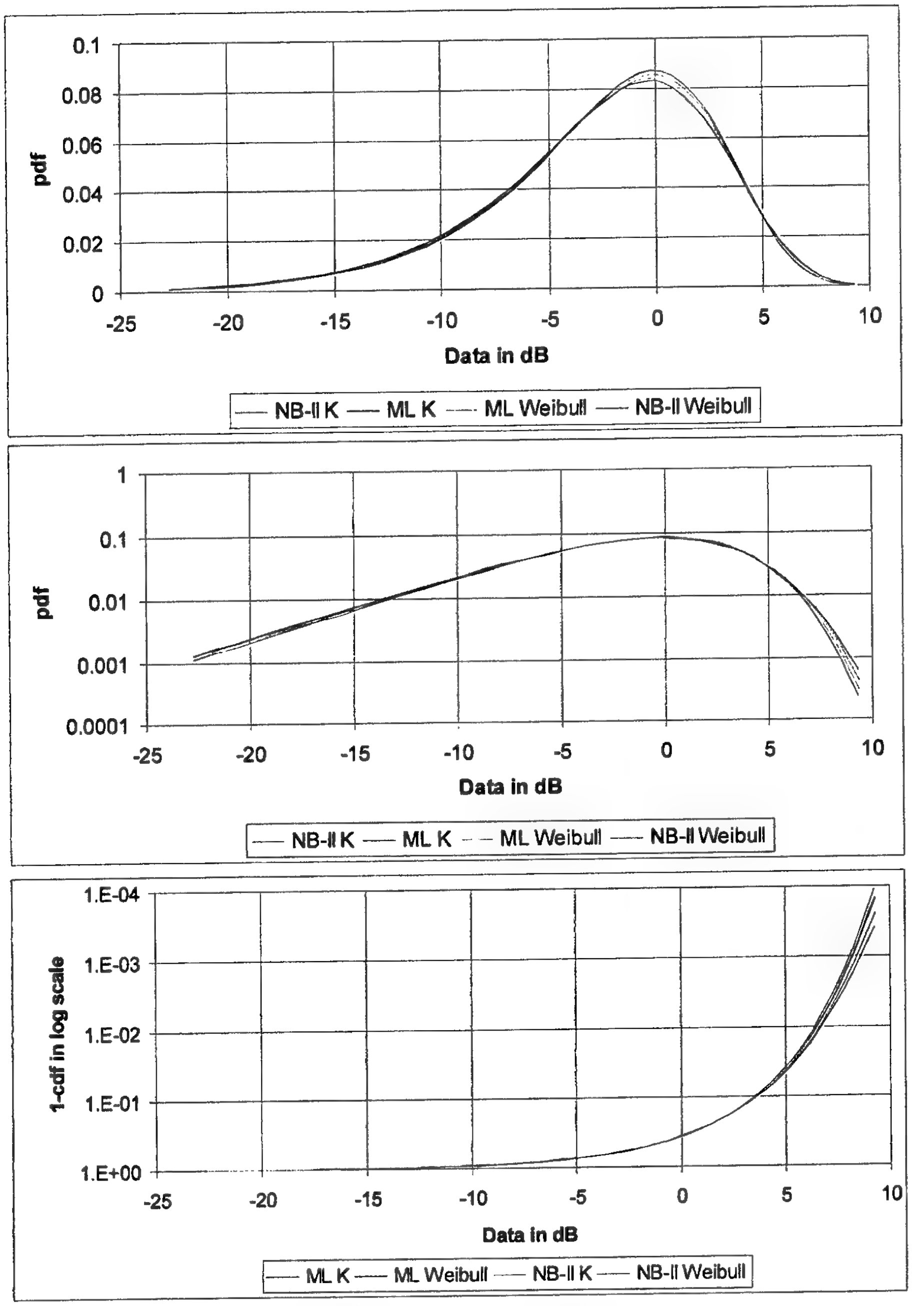

Figure 8: Comparison between the Weibull and K- distributions using the MCARM RAR L-band VV clutter data of homogenous farmland. The K-distribution converges a little bit slower.

5.2 AirSAR Single-Look L-band VV Data of Homogenous Clutter

SAR synthesises the length of radar antenna to improve the azimuth resolution. If a RAR system had the same frequency, polarisation, resolution and SNR as that of a SAR system, the collected data would be statistically the same. In this case study we analyse a block of the AirSAR single-look L-band VV data, representing the clutter of a statistically homogenous open woodland of native eucalyptus. The incidence angle of the block is about 35-45°, well within the plateau region of the grazing angle for forests. The clutter can be considered as independent of incidence angle (Dong, 2003). The variation is therefore purely spatial. The block consists of 375x336 pixels, enough sample numbers for deriving reliable statistics. The pixel size is about 3.6x6.7 m². The data was processed by JPL back in 1993 as non-standard single-look data (contrast to the standard multi-look data).

The parameters estimated by the ML and NB-I and NB-II schemes are given in Table 6. The corresponding cdfs and pdfs for the Weibull and K- distributions are shown in Figure 9 and Figure 10, respectively. The distribution is again very close to the Rayleigh distribution. The differences among all the estimates for the Weibull and K-distributions, respectively, are very small and the pdfs and cdfs plotted using these estimates are nearly identical.

The comparison between the Weibull and the K- distributions are shown in Figure 11. As can be expected, the K- distribution converges a little bit slower.

Table 6: Comparison of parameter estimation schemes for AirSAR single-look L-VV data.

Distribution	ML estimates	No-bias estimates	
		Scheme I	Scheme II
Weibull	$\hat{a} = 1.0243$ $\hat{c} = 2.4536$	$\hat{a} = 1.0097$ $\hat{c} = 2.4947$	$\hat{a} = 1.0197$ $\hat{c} = 2.4583$
K-	$\bar{x} = 0.4030$ $\hat{\alpha} = 23.7554$	N/A	$\bar{x} = 0.4030$ $\hat{\alpha} = 25.3648$

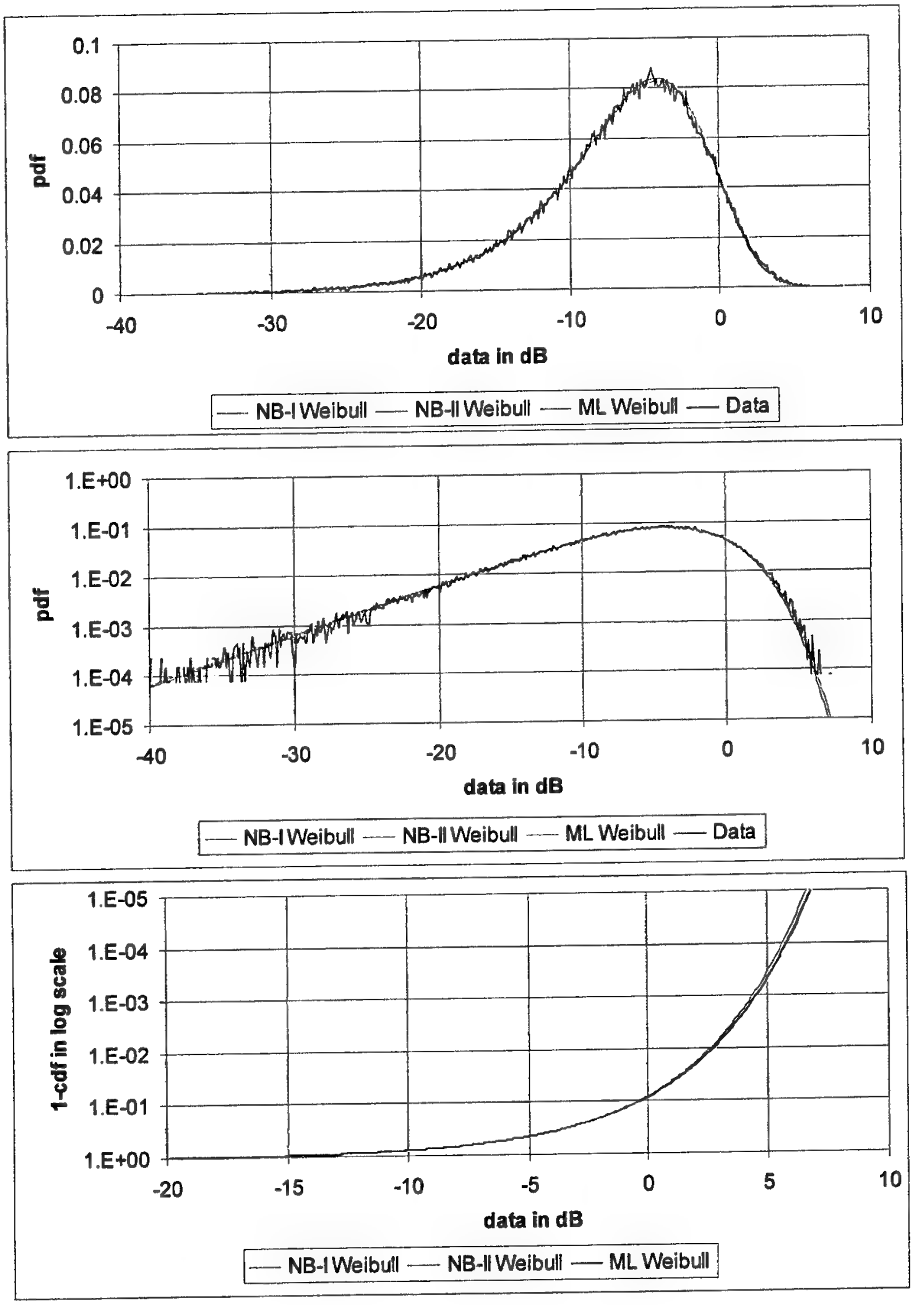

Figure 9: Comparison of parameter estimation schemes for the Weibull distribution using the AirSAR single-look L-band VV clutter data of homogenous open forests.

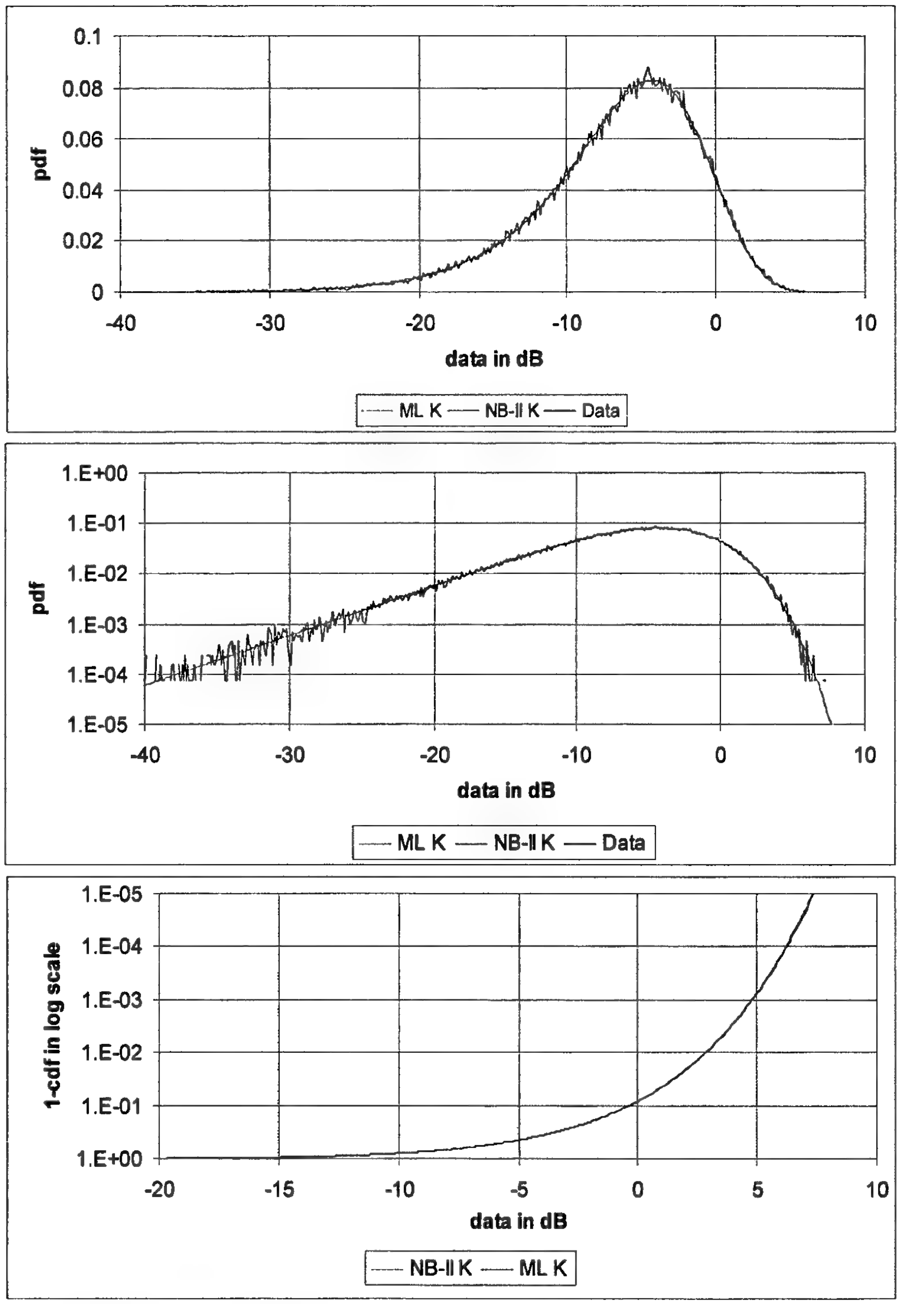

Figure 10: Comparison of parameter estimation schemes for the K- distribution using the AirSAR single-look L-band VV clutter data of homogenous open forests.

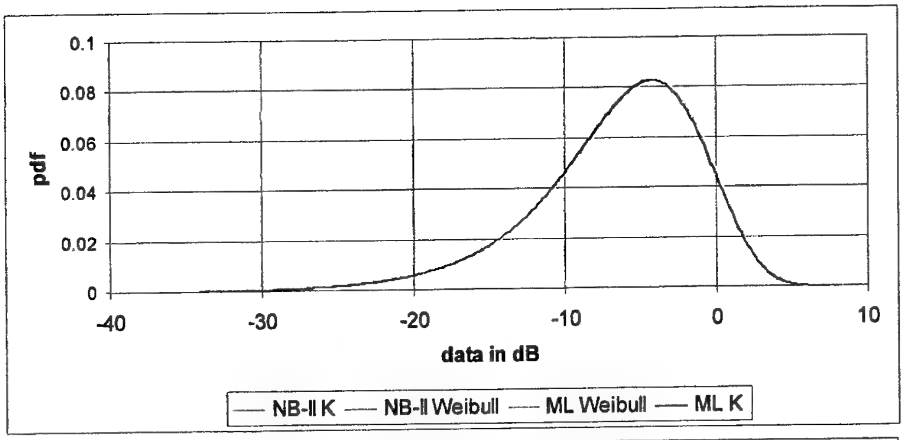

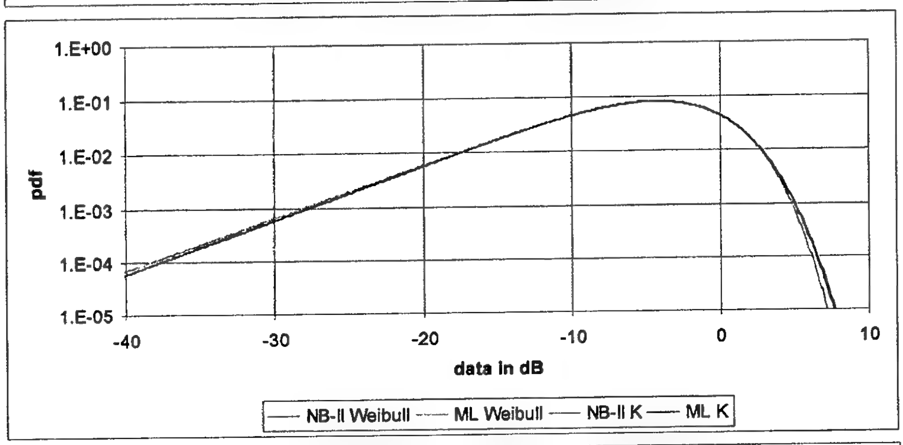

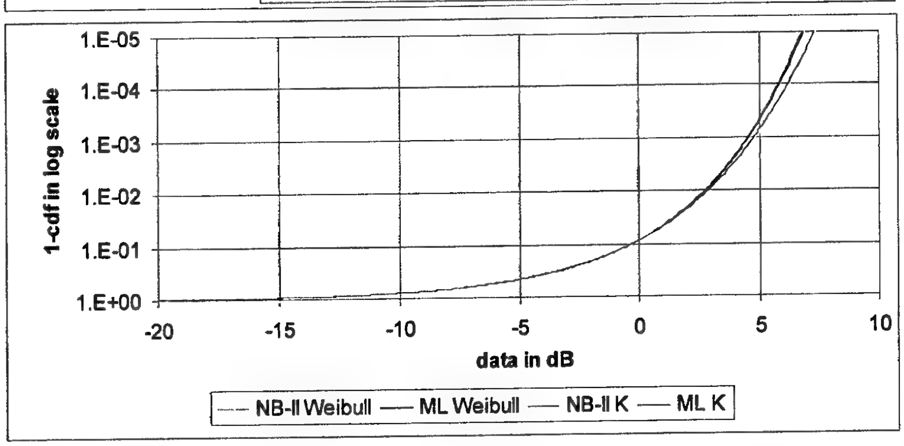

Figure 11: Comparison between the Weibull and the K- distributions for the AirSAR L-band VV clutter of homogenous open woodland of native eucalyptus. Both the ML estimates and the NB-II estimates provide the nearly identical pdf and cdf for the Weibull and the K-distributions, respectively. The convergence of the K-distribution is a little bit slower.

5.3 AirSAR Single-Look C-band VV Data of Heterogeneous Clutter

In this case study we analyse a block of the AirSAR single-look C-band VV data. Instead of selecting homogenous clutter, we deliberately select a block containing open eucalypt woodland, farmland and scattered farmhouses. The block consists of 300x400 pixels, enough sample numbers for deriving reliable statistics. The size of the pixel is the same as the AirSAR L-band data.

The parameters calculated using the ML, NB-I and NB-II schemes are given in Table 7. Since the clutter is not homogenous, the distribution becomes broader. This might be considered as the sum of the two Rayleigh distributions with a few dB mean difference. The corresponding pdfs and cdfs for the Weibull and K- distributions, respectively, are shown in Figure 12 and Figure 13. For the Weibull distribution the NB-I scheme does not produce as good estimates as the NB-II scheme in this case. The difference between the cdfs of the ML and NB-I estimates grows to about 1dB when the cdf reaches 0.9999. The difference between the ML and NB-II estimates for both the Weibull and the K-distributions, respectively, however is again insignificant, and the corresponding pdfs and cdfs are nearly identical.

The comparison between the Weibull and the K- distributions are shown in Figure 14. Since the distribution widens, but the parameter a of the Weibull distribution is still in the range of $1 < a < 2$, the convergence of the K-distribution is slower than that of the Weibull distribution.

Table 7: Comparison of parameter estimation schemes for the AirSAR single-look C-VV data of heterogeneous clutter.

Distribution	ML estimates	No-bias estimates	
		Scheme I	Scheme II
Weibull	$\hat{a} = 1.2009$ $\hat{c} = 2.8894$	$\hat{a} = 1.1312$ $\hat{c} = 3.1324$	$\hat{a} = 1.1855$ $\hat{c} = 2.8953$
K-	$\bar{x} = 0.3100$ $\hat{\alpha} = 2.7389$	N/A	$\bar{x} = 0.3100$ $\hat{\alpha} = 2.7035$

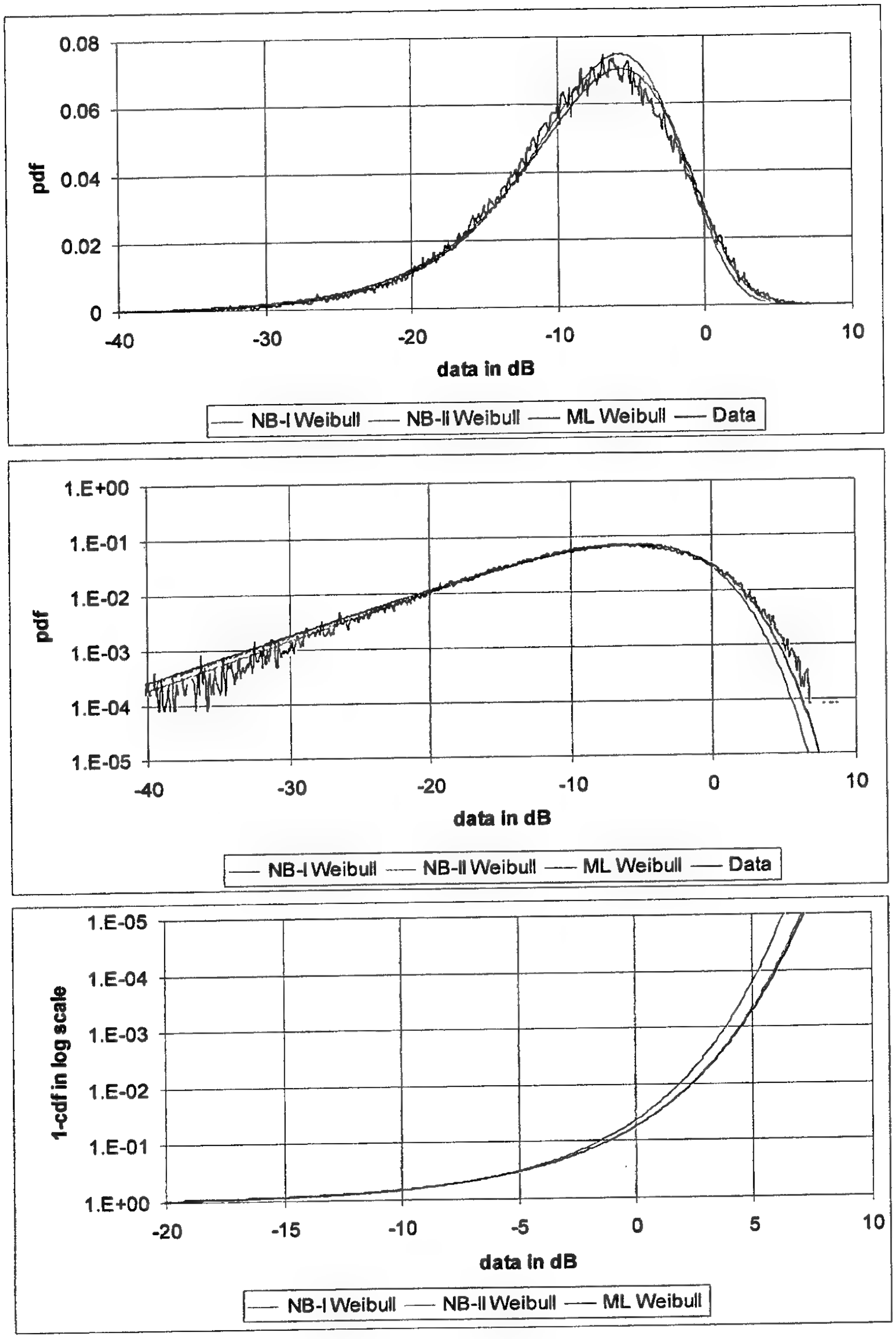

Figure 12: Comparison of the estimation schemes for the Weibull distribution using the AirSAR single-look C-band VV data of heterogenous clutter. The NB-I estimates are not as good as the NB-II estimates.

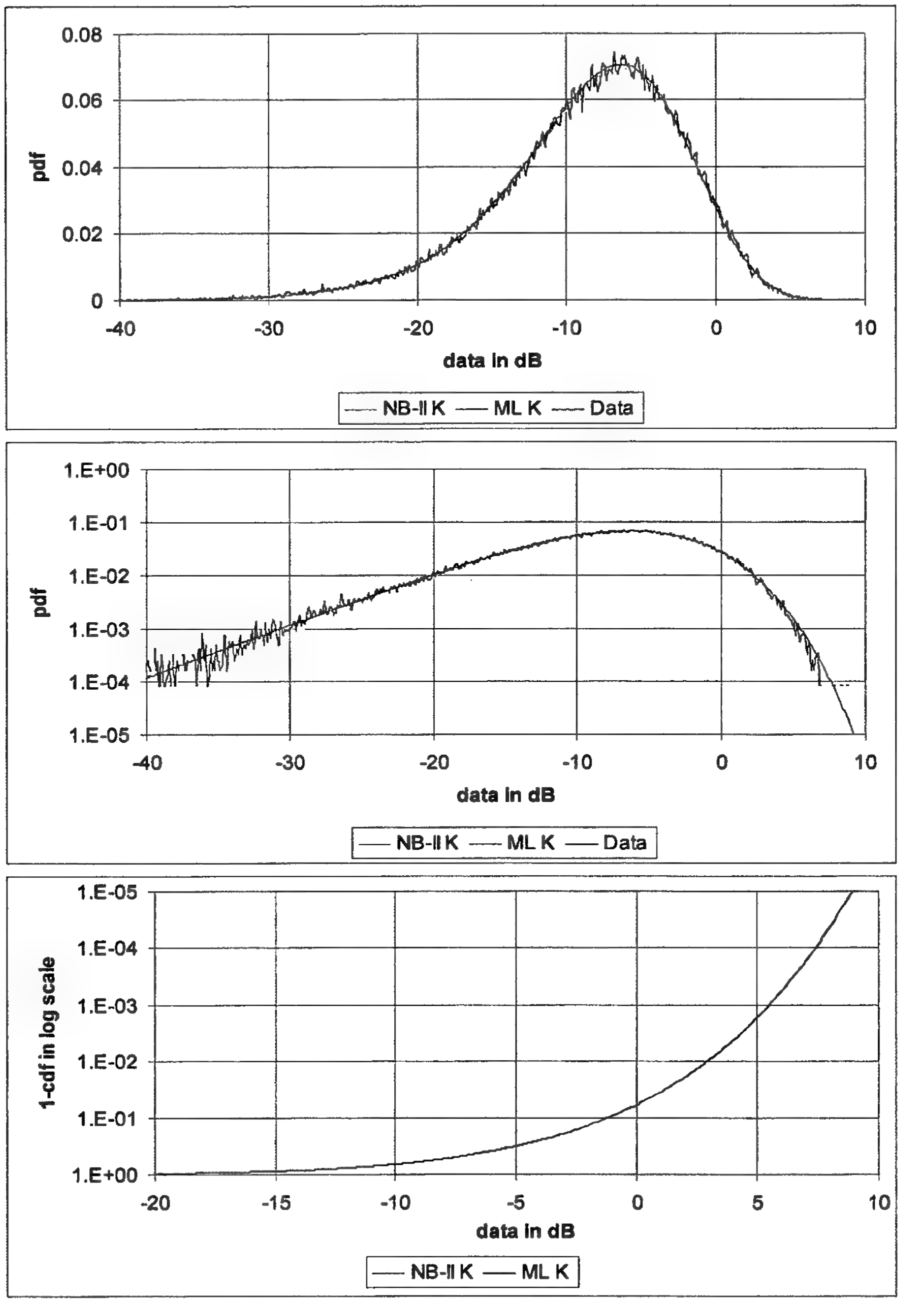

Figure 13: Comparison of the estimation schemes for the K-distribution using the AirSAR single-look C-band VV data of heterogenous clutter.

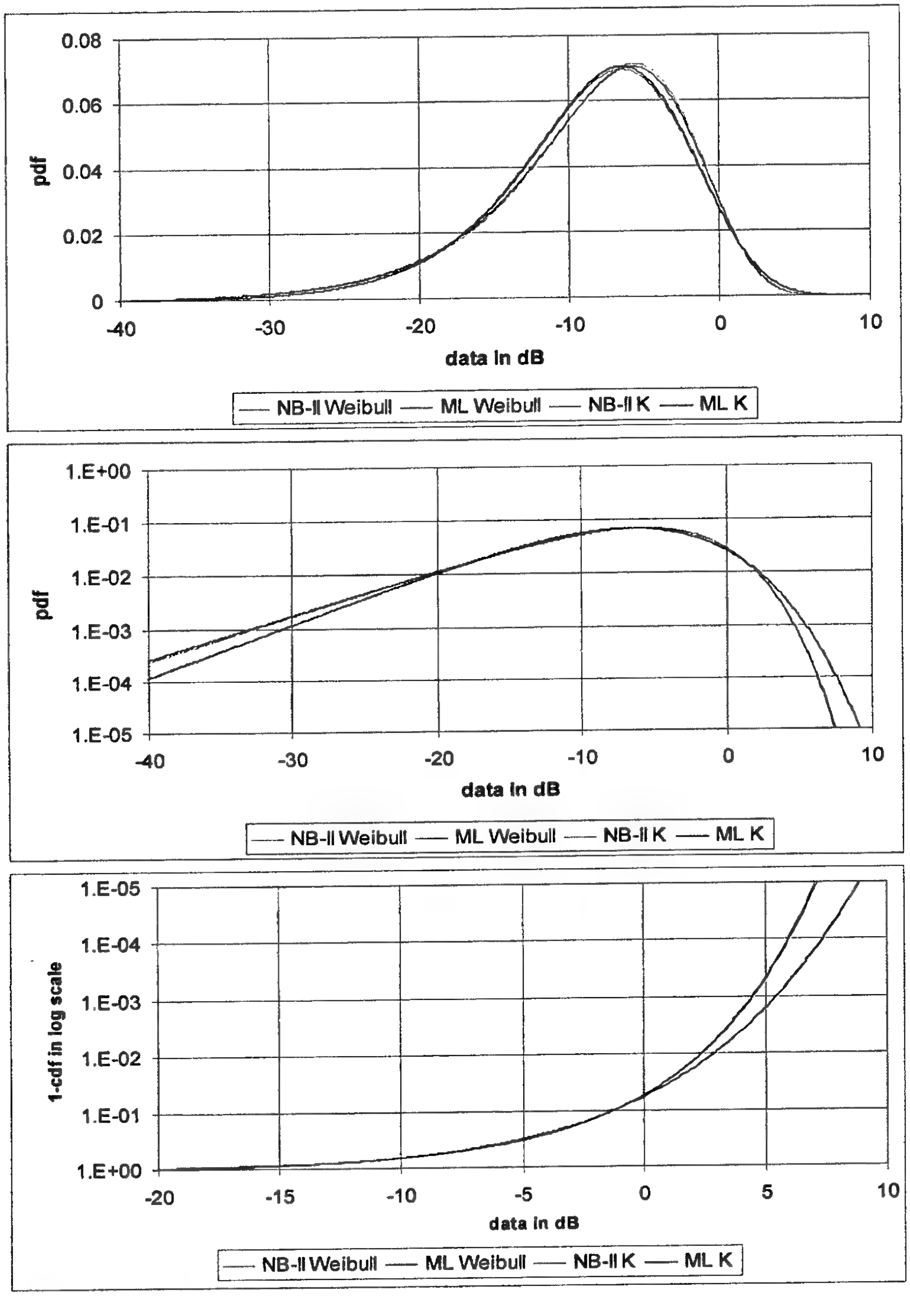

Figure 14: Comparison between the Weibull and the K- distributions for the AirSAR single-look C-band VV data of heterogonous clutter. The convergence of the K- distribution is much slower.

5.4 High Resolution Radar X-band VV Data

The data was collected by a surface-mounted X-band (centre frequency of 9750 MHz) VV polarised radar with a range resolution of 0.3 m and PRF of 1000 Hz at a grazing angle of approximate zero degrees looking at the sea surface. The original data set consists of 6000 pulses by 830 range bins. The range of the first bin is 5425.5 m. The change in range for other range bins is therefore insignificant, so the received power can be considered as independent of range, and its variation can be considered to be purely due to the spatial and temporal distribution. The data collected in the corresponding range bins for the consecutive pulses are often highly correlated and cannot be considered as independent samples. The correlation between pulse i and pulse j is defined as (Proakis and Manolakis, 1996),

$$\rho_{ij} = \frac{\sum_{k=1}^{q} u_{ik} u_{jk}^{*}}{\left[\sum_{k=1}^{q} u_{ik} u_{ik}^{*} \sum_{k=1}^{q} u_{jk} u_{jk}^{*} \right]^{1/2}} \tag{29}$$

where * denotes complex conjugate, u_{ik} is the radar's ith pulse measurement in range bin k, and q is the total number of range bins.

Figure 15 shows the correlation between the data collected in pulse 1 and the following pulses. It is safe to say that when the interval of pulses is greater than about 300 (300 milliseconds), the data become effectively uncorrelated. In our calculation, an interval of 300 pulses was used, so the data collected for pulse 1, 301, 601, ..., and 5701 were treated as independent samples given a total sample number to be $6000/300 \times 830 = 16600$. It is worth noting that the variation of the selected data is both spatial and temporal.

The mean of the data was normalised to 1 (0dB). The distribution was found significantly different from the previous cases and close to a lognormal distribution. This might be due to the illumination geometry of high resolution and low grazing angle. A high resolution means that an illuminated patch does not contain many distributed but a few discrete scatterers while a low grazing angle creates effects of shadowing and multipath propagation. Therefore the criterion of Rayleigh distribution does not hold. The pdfs of the data as well as the ML lognormal, Weibull and K-distribution curve fitting are shown in Figure 16. It can be seen that the pdf of the data is not quite a lognormal distribution, but among the three distributions, the lognormal distribution is the best to fit the data. The ML lognormal distribution is even a little conservative at the high end (the disagreement in the low end might be due to the noise level of the radar) which can be further identified by viewing the cdfs of the data and the ML lognormal curve fitting as shown in Figure 17.

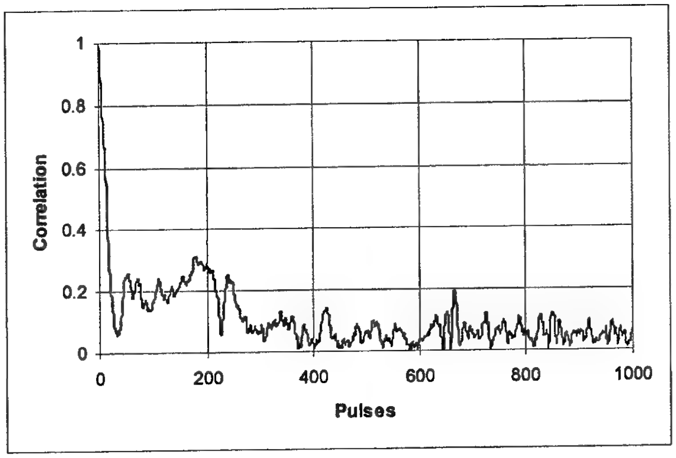

Figure 15: Data correlation is a function of the interval of pulses.

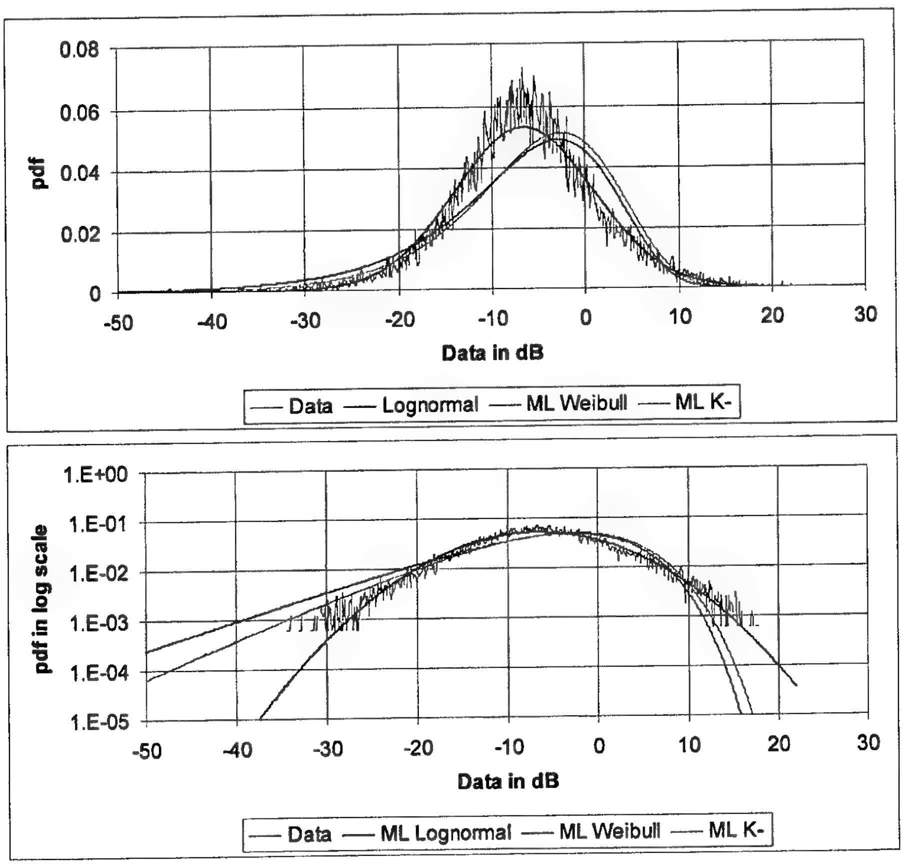

Figure 16: Pdfs of the data as well as the ML estimated lognormal, Weibull and K- distribution curve fitting.

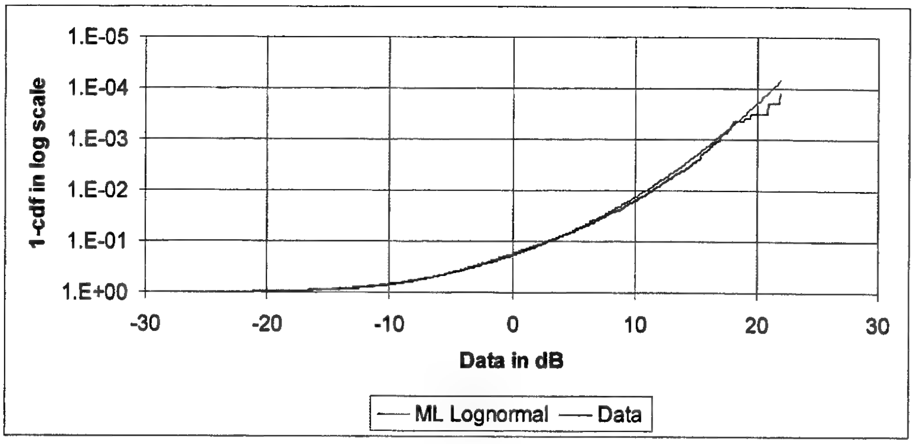

Figure 17: Cdfs of the data and the ML estimated lognormal curve fitting. Since the true data distribution is not quite a lognormal distribution, the ML estimates are a little conservative at the high end.

The ML estimated parameters for the three distribution functions are given in Table 8. However, it has to be pointed out that pdf parameters of sea clutter are highly dependent on radar frequency, polarisation, grazing angle, as well as weather conditions.

Table 8: The ML estimated parameters for the lognormal, Weibull and K- distributions for the approximate zero degree grazing angle, high resolution X-band VV sea clutter data (the mean of the data has been normalised to 1).

Distribution function	Parameters
Lognormal	$\mu = -1.4892$; $s = 1.7207$
Weibull	$b = 0.5799$; $c = 1.4453$
K-	$\bar{x} = 1.0$; $\alpha = 0.8080$

6. Conclusions

The Weibull, K- and lognormal distributions, widely used to represent radar clutter distributions, have been studied.

Since clutter is often expressed in the dB, its pdf and cdf are also plotted on the dB scale, the statistical properties including mean and variance for the Weibull and K-distributions in the log domain have been derived. These values are later used for parameter estimations.

If the clutter is modelled as a Weibull distribution, the shape parameter a is generally in the range of $1 < a < 2$. Corresponding to this range, the lognormal distribution converges slowest among the three distributions, followed by the K-distribution, and

the Weibull distribution converges fastest. This finding contradicts a general claim of Billingsley (2002) that the K-distribution converges faster than the Weibull distribution. In fact his claim is true only when the distributions correspond to $a > 2$.

However, the value of a generally becomes larger if the grazing angle is low and the resolution is high. The value of a ranging from 1.8 to 5.4 for data of various terrain types including urban and forests, with the grazing angle less than 2° and resolution in the order of $10^3 m^2$, has been reported (Billingsley, 2002). If the resolution reduces to $10^6 m^2$, the value of a becomes 1.1 to 2.8 (Billingsley, 2002).

According to both the RAR and SAR data analysed, visually the K-distribution seems marginally better than the Weibull distribution in describing the clutter distribution especially at the high end of the distribution. We did not use the standard or modified statistical tests such as the chi-square or modified chi-square tests (Antipov, 1998, Chan, 1990) to numerically test which distribution is better. Because we are only concerned about the distribution at the high end, the error occurring in other parts of the distribution should not be significant for this programme.

Theoretically, if the surface is homogenous and contains many scatterers, the distribution of the radar clutter is Rayleigh. Both the RAR and SAR data analysis support this theory. The radar resolution of the RAR data is of the order of tens of thousand square metres whereas the resolution of the AirSAR single-look data is of the order of tens of square metres, but both data approach the Rayleigh distribution for homogenous clutter. For heterogenous areas, the clutter distribution is broader than the Rayleigh distribution. This can be considered as the sum of two or more Rayleigh distributions with slightly different means. The distribution of sea clutter of very fine resolution and low grazing angle is approximately lognormal, according to the data analysed. At low grazing angle, the shadowing and multipath propagation effect may dominate so the Rayleigh criterion does not hold.

Parameter estimation is an important issue and the ML estimates are the optimal. Previous research concentrated on using the Lagrange method to find the ML estimates. For the K-distribution because the derivative of the embedded Bessel function cannot be expressed in a closed form, it is very difficult to find the ML estimates using the Lagrange method, if not impossible. This report has proposed a direct method to find the ML estimates for the K-distribution. The direct method does not require the derivative of the Bessel function.

The ML method provides the optimal parameter estimates. Unfortunately, except for the lognormal distribution, the ML estimates for both the Weibull and K- distribution involve iterative computation manipulating sample data. Faster estimations are desirable in real-time data processing. This report has proposed two no-bias estimation schemes, namely NB-I estimates and NB-II estimates. The NB-I scheme uses the mean and the variance of data in the log domain to calculate the parameters (so the estimated mean and variance equal the mean and variance of the data in the log domain), while

the NB-II scheme uses the mean of the data in the linear domain (arithmetic mean) and the mean of the data in the log domain (geometric mean) to calculate the parameters (so the estimated means equal the means of the data in the linear and log domains, respectively). It has been found that NB-II performs better, as the estimation only uses the first moment of the data. The differences between the NB-II estimates and the ML estimates are insignificant, and the corresponding pdfs and cdfs are nearly identical for all cases studied. The accuracy of the NB-I is not as good as that of NB-II, though the difference is still small.

7. Acknowledgement

The author thanks Drs J Whitrow and A Shaw for their various discussions and comments, and Mr S Capon for his administrative support. The comments and corrections from the Vetting Officer, Mr J Baldwinson, improved the readability of the report.

8. References

1. Antipov, I, "Analysis of sea clutter data," Technical Report, *DSTO-TR-0647*, Defence Science Technology Organisation, Australia, 1998.

2. Billingsley, J B, *Low-Angle Land Clutter Measurements and Empirical Models*, William Andrew Publishing, 2002.

3. Blacknell, D, "Comparison of parameter estimators for K-distribution," *IEE Proc~ Radar, Sonar and Navigation*, vol. 141, no. 1, pp. 45-52, 1994.

4. Chan, H C, "Radar sea clutter at low grazing angles," *IEE Proceedings Pt F*, vol. 137, no. 2, pp. 102-112, 1990.

5. Davidson, G, Griffiths, H D, and Ablett, A, "Statistical analysis of high resolution land clutter," *Proceedings of International Conference on Radar 2002*, 15-17 Oct 2002, Edinburgh, UK.

6. Dong, Y, "L-band VV clutter analysis for natural land," *Proceedings of International Conference on Radar 2003*, 3-5 September 2003, Adelaide, Australia.

7. Farina, A, Gini, F, Greco, M V, and Verrazzani, L, "High resolution sea clutter data: statistical analysis of recorded live data," *IEE Proc~ Radar Sonar and Navigation*, vol. 144, no. 3, pp. 121-130, 1997.

8. Gini, F, Giannakis, G B, Greco, M, and Zhou, G T, "Time-average subspace methods for radar clutter texture retrieval," *IEEE Trans on Signal Processing*, vol, 49, no. 9, pp. 1886-1898, 2001.

9. Gini, F, and Greco, M, "Texture modelling, estimation and validation using measured sea clutter data," *IEE Proc~ Radar Sonar and Navigation,* vol. 149, no. 3, pp. 115-124, 2002.

10. Gradshteyn, I S, and Ryzhik, I M, *Tables of Integrals, Series and Products,* Academic Press, 1980.

11. Jao, J K, "Amplitude distribution of composite terrain radar clutter and the K-distribution," *IEEE Trans on Antennas and Propagation,* vol. AP-32, no. 10, pp. 1049-1062, 1984.

12. Joughin, I R, Percival, D B, and Winebrenner, D P, "Maximum likelihood estimation of K distribution parameters for SAR data," *IEEE Trans on Geoscience and Remote Sensing,* vol. 31, no. 5, pp 989-999, 1993.

13. Long, M W (editor), *Airborne Early Warning System Concepts*, Artech House, 1992.

14. Long, M W, *Radar Reflectivity of Land and Sea,* 3rd Edition, Artech House, 2001.

15. Menon M V, "Estimation of the shape and scale parameters of the Weibull distribution," *Technometrics,* vol. 5, no. 2, pp. 175-182, 1963.

16. Oliver, C J, "Optimum texture estimators for SAR clutter," *Journal of Physics D: Applied Physics*, vol. 26, pp. 1824-1835, 1993.

17. Proakis, J G, and Manolakis, D G, *Digital Signal Processing,* 3rd Edition, Prentice-Hall Inc, 1996.

18. Raghavan, R S, "A method for estimating parameters of K-distributed clutter," *IEEE Trans on Aerospace and Electronic Systems,* vol. 27, no. 2, pp. 238-246, 1991.

19. Ward, K D, Baker, C J, and Watts, S, "Maritime surveillance radar Part I: Radar scattering from the ocean surface," *IEE Proceedings, Pt F*, vol. 137, no. 2, pp. 51-62, 1990.

20. Watts, S, "Radar detection prediction in sea clutter using the compound K-distribution model," *IEE Proceedings, Pt F*, vol 32, no. 7, pp. 613-620, 1985.

21. Watts, S, "Radar detection prediction in K- distributed sea clutter and thermal noise," *IEEE Trans on Aerospace and Electronic Systems*, vol. AES-23, no. 1, pp. 40-45, 1987.

22. Wolfram Research Inc, *Mathematica,* Version 4, 2000.

Appendix A: Statistics of Weibull and K-Distributions in Log Domain

In order to maintain the physical meaning, generally radar signals such as power, RCS and reflectivity are manipulated in the linear domain, though their values are often expressed in dB. For instance, the average power of 0 dBw (1 w) and 10 dBw (10 w) is 7.4 dBw (5.5 w) but not 5 dBw (3.16 w), unless specified. However, if we define the manipulation domain, we may accept 7.4 dBw as the arithmetic mean and 5dBw as the geometric mean. Without loss of generality, we define the mean or more precisely the arithmetic mean as,

$$\bar{x}_{arith} = \frac{1}{n}\sum_{i=1}^{n} x_i \tag{A1}$$

Similarly we may define the geometric mean as,

$$\bar{x}_{geom} = \left(\prod_{i=1}^{n} x_i\right)^{1/n} \qquad x_i > 0 \tag{A2}$$

When the value of x_i is expressed in dB, (A2) is equivalent to as,

$$\bar{z} = \frac{1}{n}\sum_{i=1}^{n} z_i \tag{A3}$$

where $z = 10\log x$.

Therefore we may consider the manipulation in the linear domain as the arithmetic manipulation and the manipulation in the log domain as the geometric manipulation. Since radar signals are often expressed in the dB domain, the geometric manipulation sometimes may have advantages. This Appendix derives statistics for the Weibull and the K- distributions in the log domain. The statistics of the lognormal distribution in the log domain is simply the statistics of a normal distribution.

A.1. Statistics of Weibull Distribution in Log Domain

The pdf of the Weibull distribution in the natural logarithmic domain is,

$$p(y) = bc\left(e^{y}\right)^{b} \exp\left(-c\left(e^{y}\right)^{b}\right) \qquad -\infty < y < \infty \tag{A4}$$

where $y = \ln x$.

To find the mean and variance of the distribution requires the evaluation of the first and the second moment of the distribution,

$$E(y) = \int_{-\infty}^{\infty} y p(y) dy \tag{A5}$$

$$E(y^2) = \int_{-\infty}^{\infty} y^2 p(y) dy \tag{A6}$$

Let $t = c(e^y)^b$, we have

$$E(y) = \frac{1}{b}\left[-\ln c + \int_0^{\infty} \ln t \, e^{-t} dt\right] \tag{A7}$$

$$E(y^2) = \frac{1}{b^2}\left[\ln^2 c + \int_0^{\infty} \ln^2 t \, e^{-t} dt - 2\ln c \int_0^{\infty} \ln t \, e^{-t} dt\right] \tag{A8}$$

According to Gradshteyn and Ryzhik (1980), and Mathemetica, Version 4 (Wolfram Research, 2000) we can evaluate the special integrals in (A7) and (A8) as,

$$\int_0^{\infty} \ln t \, e^{-t} dt = -\psi^{(0)}(1) = \gamma \tag{A9}$$

where $\psi^{(n)}(x)$ is the Polygamma function, defined as the n^{th} derivative of the logarithm of the Gamma function, $\frac{d^{n+1}}{dx^{n+1}}(\ln \Gamma(x))$ and γ is Euler's Gamma constant.

$$\int_0^{\infty} \ln^2 t \, e^{-t} dt = \gamma^2 + \frac{\pi^2}{6} \tag{A10}$$

Finally we have,

$$E(y) = -\frac{1}{b}(\gamma + \ln c) \tag{A11}$$

$$\mathrm{var}(y) = E(y^2) - E^2(y) = \frac{\pi^2}{6b^2} \tag{A12}$$

In the dB domain, the above expressions become,

$$E(z) = -\frac{k_0}{b}(\gamma + \ln c) \tag{A13}$$

$$\mathrm{var}(z) = \frac{k_0{}^2\pi^2}{6b^2} \tag{A14}$$

where $k_0 = 10/\ln 10$

A.2. Statistics of K- Distribution in Log Domain

The pdf of the K- distribution in the natural logarithmic domain is,

$$p(y) = \frac{2}{\Gamma(\alpha)}\left(\frac{\alpha}{\bar{x}}e^y\right)^{\frac{\alpha+1}{2}} K_{\alpha-1}\left(2\sqrt{\frac{\alpha}{\bar{x}}e^y}\right) \qquad -\infty < y < \infty \tag{A15}$$

Letting $t = 2(\alpha e^y / \bar{x})^{1/2}$, we have

$$E(y) = \frac{1}{\Gamma(\alpha)2^{\alpha-1}}\int_0^\infty (2\ln t + \ln\frac{\bar{x}}{4\alpha})\, t^\alpha K_{\alpha-1}(t)dt \tag{A16}$$

$$E(y^2) = \frac{1}{\Gamma(\alpha)2^{\alpha-1}}\int_0^\infty (2\ln t + \ln\frac{\bar{x}}{4\alpha})^2\, t^\alpha K_{\alpha-1}(t)dt \tag{A17}$$

Evaluations of the special integrals in (A16) and (A17) include (Gradshteyn and Ryzhik, 1980, Mathemetica, Version 4, 1998),

$$\int_0^\infty t^\alpha K_{\alpha-1}(t)dt = 2^{\alpha-1}\Gamma(\alpha) \tag{A18}$$

$$\int_0^\infty t^\alpha \ln t\, K_{\alpha-1}(t)dt = 2^{\alpha-2}\Gamma(\alpha)\left[-\gamma + 2\ln 2 + \psi^{(0)}(\alpha)\right] \tag{A19}$$

$$\begin{aligned}&\int_0^\infty t^\alpha \ln^2 t\, K_{\alpha-1}(t)dt \\ &= 2^{\alpha-4}\Gamma(\alpha)\left[2\gamma^2 + \frac{\pi^2}{3} - 8\gamma\ln 2 + 8\ln^2 2 - 4(\gamma - 2\ln 2)\psi^{(0)}(\alpha) + 2(\psi^{(0)}(\alpha))^2 + 2\psi^{(1)}(\alpha)\right]\end{aligned} \tag{A20}$$

Finally we have,

$$E(y) = -\gamma + \psi^{(0)}(\alpha) - \ln\alpha + \ln\bar{x} \tag{A21}$$

$$\mathrm{var}(y) = \psi^{(1)}(\alpha) + \frac{\pi^2}{6} \tag{A22}$$

In the dB domain, the above expressions become as,

$$E(z) = k_0\left(-\gamma + \psi^{(0)}(\alpha) - \ln\alpha + \ln\bar{x}\right) \tag{A23}$$

$$\mathrm{var}(z) = k_0^{\,2}\left[\psi^{(1)}(\alpha) + \frac{\pi^2}{6}\right] \tag{A24}$$

We have proven in Section 2.2 that the K- distribution with $\alpha = 1/2$ is identical to the Weibull distribution with $b = 1/2$ and $c = (2/\bar{x})^{1/2}$. In fact,

$$\psi^{(0)}(1/2) = -\gamma - 2\ln 2 \tag{A25}$$

$$\psi^{(1)}(1/2) = \pi^2/2 \tag{A26}$$

We can see that the statistics of the Weibull and K- distributions are indeed the same with these special conditions.

Appendix B: RAR Data Pre-processing for Spatial Distribution Analysis

According to the radar equation, the received power from terrain is,

$$P_r = \frac{P_{avg} G_t G_r \lambda^2 \sigma_0 F^4 A_g}{(4\pi)^3 R^4 L} \tag{B1}$$

where P_{avg} - average transmitted power, G_t and G_r - gains of radar transmitting and receiving antenna in the direction, λ - wavelength, A_g - resolvable area of the ground, R - range of the ground patch, σ_0 - reflectivity, F^4 - the pattern propagation factor and L the total loss including propagation loss and system loss.

In order to analyse the spatial distribution of clutter, $\sigma_0 F^4$, we need to pre-process the received power in such a way to extract $\sigma_0 F^4$. This is done in two steps. First we calculate the clutter that is only a function of grazing angle. Secondly we truncate those data which are highly correlated to the grazing angle. The distribution of the remaining data, which are independent of (almost uncorrelated to) the grazing angle, therefore can be considered as the spatial distribution.

For a given range, the area illuminated by the 3dB main beamwidth can be written as,

$$A_g = r \Delta r \phi_{3dB} \tag{B2}$$

where $r \approx R\cos\theta$, θ is the depression angle; $\Delta r = \frac{\tau c}{2\cos\beta}$, β is the grazing angle and τ is the time interval between two consecutive range bins. For the MCARM system, the height of the aircraft is about 3500 m, $\tau = 0.8\mu s$. With these parameters, and noting the grazing angle is very low, so $\cos\theta \approx \cos\beta$, the ground resolution is in the order of $8 \times 10^5 m^2$, a very coarse resolution for the analogue sum channel.

Assuming the clutter in the 3dB main beamwidth area to be constant, we have,

$$P_{r3dB} \propto \frac{\sigma_0 F^4}{R^3} \int_{\phi_{3dB}} G_t(\theta,\phi) G_r(\theta,\phi) d\phi \tag{B3}$$

where P_{r3dB} is the power received from the area illuminated by the main beam of 3dB beamwidth. When radar looks at boardside, the Doppler resolution is in the azimuth

direction. Therefore, after the received power being transformed into the Doppler frequency domain, the corresponding component of P_{r3dB} can be determined. The Doppler frequency shift due to the movement of vegetation at L-band is relatively small (Billingsley, 2002), and the main contribution to the Doppler frequency shift is therefore due to the geometry.

$$P_{r3dB} = \sum_{f=f_1}^{f_2} P(f) \qquad \text{(B4)}$$

where $P(f)$ is the power component of the frequency f and

$$f_1 = \frac{2v}{\lambda}\cos\theta\cos\left(\frac{\pi}{2}+\frac{\phi_{3dB}}{2}-\delta_0\right) \qquad \text{(B5)}$$

$$f_2 = \frac{2v}{\lambda}\cos\theta\cos\left(\frac{\pi}{2}-\frac{\phi_{3dB}}{2}-\delta_0\right) \qquad \text{(B6)}$$

where v is the velocity of the platform, θ the depression angle, δ_0 the drift angle of the platform and ϕ_{3dB} the azimuth angle of 3dB beamwidth.

We then have the final expression,

$$\sigma_0 F^4 \propto \frac{P_{r3dB} R^3}{G^2(\theta)} \qquad \text{(B7)}$$

where

$$G^2(\theta) = \int_{\phi_{3dB}} G_t(\theta,\phi) G_r(\theta,\phi) d\phi \qquad \text{(B8)}$$

The above integration is along the contour of constant-elevation, which also assumes the range on the contour of constant-elevation is the same. Rigorously speaking, the contour of constant elevation angle of a tilt antenna array on the ground is nearly a straight line whereas the contour of the equal-range is a half-circle. However, we can consider the two contours to be coincident for a small angle of ϕ_{3B}.

The result of (B7), the clutter as a function of grazing angle is shown in Figure B1. Apart from the notch which corresponds to the clutter of bay water, the clutter shown in the figure is of low relief farmland. The clutter of farmland seems to be independent of grazing angle when the angle is grater than 5°, and the variation can be considered as the random process of clutter in space. As shown in Figure B2 range bins 200-316 (because of the transmitter signal leakage in range bin 68, signals in range bins of 1-200 are not used) satisfy this criterion of $\theta \geq 5^o$. This provides a total of 127 samples, too less for the spatial distribution analysis.

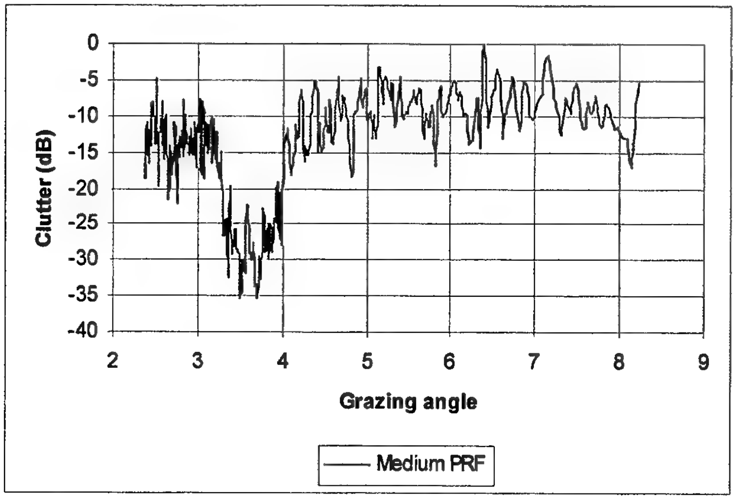

Figure B1: Clutter as a function of grazing angle. The notch corresponds to clutter of bay water and the others to farmland.

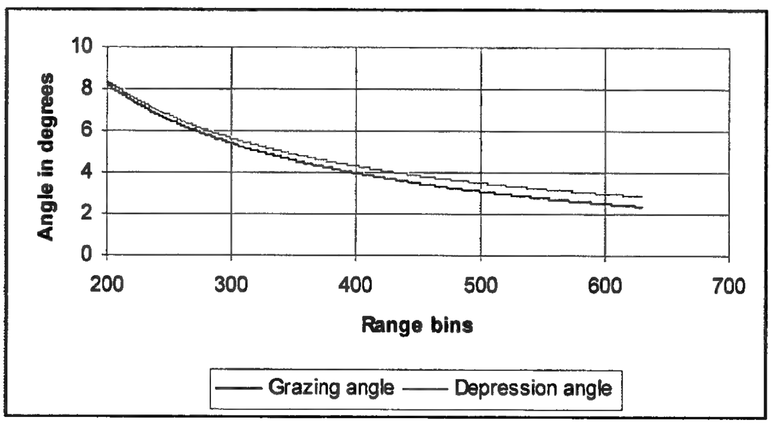

Figure B2: Grazing angle and depression angle as functions of range bins.

The pulse number in the CPI process of the medium PRF MCARM data is 128. Unfortunately the corresponding samples collected in different pulses are generally highly correlated, and therefore are not independent samples. Figure B3 shows the correlation between the corresponding samples collected from pulse 1 and pulse k ($k = 1, 2, \cdots, 128$). Correlations among other CPI pulses have the similar pattern. It can be seen that in general the samples become independent if the interval between the CPI pulses are more than 20. Therefore we have selected samples collected from pulses 1, 25, 50, 75, 100 and 125 for the distribution analysis. The total sample number is

therefore $127 \times 6 = 762$. The number is still not sufficient for distribution analysis, but this is the maximum number we can extract from one medium PRF MCARM data set.

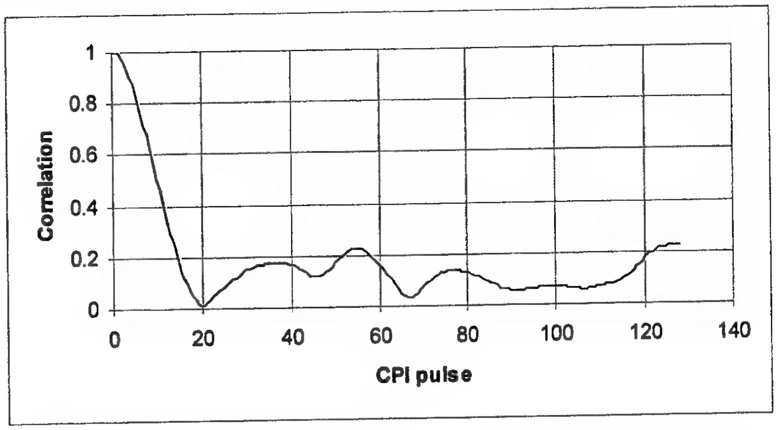

Figure B3: Signal correlation between the 1st CPI pulse and the kth CPI pulse ($k = 12, \cdots, 128$).

DISTRIBUTION LIST

Clutter Spatial Distribution and New Approaches of Parameter Estimation for Weibull and K- Distributions

Yunhan Dong

AUSTRALIA

DEFENCE ORGANISATION		**No. of Copies**
Task Sponsor		
OCAEWCSPO		1
S&T Program		
Chief Defence Scientist	shared copy	1
FAS Science Policy		
AS Science Corporate Management		
Director General Science Policy Development		
Counsellor Defence Science, London		Doc Data Sheet
Counsellor Defence Science, Washington		Doc Data Sheet
Scientific Adviser to MRDC, Thailand		Doc Data Sheet
Scientific Adviser Joint		1
Navy Scientific Adviser		Doc Data Sht & Dist List
Scientific Adviser - Army		Doc Data Sht & Dist List
Air Force Scientific Adviser		1
Scientific Adviser to the DMO M&A		1
Scientific Adviser to the DMO ELL		Doc Data Sht & Dist List
Director of Trials		1
Systems Sciences Laboratory		
Chief of Electronic Warfare and Radar Division		Doc Data Sht & Dist List
EWSTIS (Soft copy)		1
Research Leader Microwave Radar		1
Head RST, EWRD: Dr J Whitrow		1
Task Manager: Mr G Lawrie		1
Head IRS, ISRD: Dr N Stacy		1
Head RFS, WSD: Dr A Szabo		1
Mr S Capon, RST Group, EWRD		1
Dr L Powis, RST Group, EWRD		1
Mr J Baldwinson, RMA Group, ERWD		1
Author: Dr Y Dong		1
DSTO Library and Archives		
Library Edinburgh		1
Australian Archives		1

Capability Systems Division
Director General Maritime Development — Doc Data Sheet
Director General Aerospace Development — Doc Data Sheet
Director General Information Capability Development — Doc Data Sheet

Office of the Chief Information Officer
Deputy CIO — Doc Data Sheet
Director General Information Policy and Plans — Doc Data Sheet
AS Information Structures and Futures — Doc Data Sheet
AS Information Architecture and Management — Doc Data Sheet
Director General Australian Defence Simulation Office — Doc Data Sheet

Strategy Group
Director General Military Strategy — Doc Data Sheet
Director General Preparedness — Doc Data Sheet

HQAST
SO (Science) (ASJIC) — Doc Data Sheet

Navy
Director General Navy Capability, Performance and Plans, Navy Headquarters — Doc Data Sheet
Director General Navy Strategic Policy and Futures, Navy Headquarters — Doc Data Sheet

Army
ABCA National Standardisation Officer, Land Warfare Development Sector, Puckapunyal — e-mailed Doc Data Sheet
SO (Science), Deployable Joint Force Headquarters (DJFHQ) (L), Enoggera QLD — Doc Data Sheet
SO (Science) - Land Headquarters (LHQ), Victoria Barracks NSW — Doc Data & Exec Summ

Intelligence Program
DGSTA Defence Intelligence Organisation — 1
Manager, Information Centre, Defence Intelligence Organisation — 1
Assistant Secretary Corporate, Defence Imagery and Geospatial Organisation — Doc Data Sheet

Defence Materiel Organisation
Head Airborne Surveillance and Control — Doc Data Sheet
Head Aerospace Systems Division — Doc Data Sheet
Head Electronic Systems Division — Doc Data Sheet
Head Maritime Systems Division — Doc Data Sheet
Head Land Systems Division — Doc Data Sheet
Head Industry Division — Doc Data Sheet
Chief Joint Logistics Command — Doc Data Sheet
Management Information Systems Division — Doc Data Sheet
Head Materiel Finance — Doc Data Sheet

Defence Libraries	
Library Manager, DLS-Canberra	Doc Data Sheet
Library Manager, DLS - Sydney West	Doc Data Sheet
OTHER ORGANISATIONS	
National Library of Australia	1
NASA (Canberra)	1
UNIVERSITIES AND COLLEGES	
Australian Defence Force Academy	
Library	1
Head of Aerospace and Mechanical Engineering	1
Serials Section (M list), Deakin University Library, Geelong, VIC	1
Hargrave Library, Monash University	Doc Data Sheet
Librarian, Flinders University	1

OUTSIDE AUSTRALIA

INTERNATIONAL DEFENCE INFORMATION CENTRES	
US Defense Technical Information Center	2
UK Defence Research Information Centre	2
Canada Defence Scientific Information Service	1
NZ Defence Information Centre	1
ABSTRACTING AND INFORMATION ORGANISATIONS	
Library, Chemical Abstracts Reference Service	1
Engineering Societies Library, US	1
Materials Information, Cambridge Scientific Abstracts, US	1
Documents Librarian, The Center for Research Libraries, US	1
INFORMATION EXCHANGE AGREEMENT PARTNERS	
National Aerospace Laboratory, Japan	1
National Aerospace Laboratory, Netherlands	1
AFRL, Rome, NY: Dr M Davis	1
SPARES	5
Total number of copies:	**44**

Page classification: UNCLASSIFIED

DEFENCE SCIENCE AND TECHNOLOGY ORGANISATION DOCUMENT CONTROL DATA					1. PRIVACY MARKING/CAVEAT (OF DOCUMENT)
2. TITLE Clutter Spatial Distribution and New Approaches of Parameter Estimation for Weibull and K- Distributions			3. SECURITY CLASSIFICATION (FOR UNCLASSIFIED REPORTS THAT ARE LIMITED RELEASE USE (L) NEXT TO DOCUMENT CLASSIFICATION) Document (U) Title (U) Abstract (U)		
4. AUTHOR(S) Yunhan Dong			5. CORPORATE AUTHOR Systems Sciences Laboratory PO Box 1500 Edinburgh SA 5111		
6a. DSTO NUMBER DSTO-RR-0274	6b. AR NUMBER AR-013-086		6c. TYPE OF REPORT Research Report		7. DOCUMENT DATE April 2004
8. FILE NUMBER 2004/1024415	9. TASK NUMBER AIR 02/232	10. TASK SPONSOR OCAEWCSPO	11. NO. OF PAGES		12. NO. OF REFERENCES
13. URL on the World Wide Web http://www.dsto.defence.gov.au/corporate/reports/DSTO-RR-0274.pdf			14. RELEASE AUTHORITY Chief, Electronic Warfare and Radar Division		
15. SECONDARY RELEASE STATEMENT OF THIS DOCUMENT Approved for Public Release OVERSEAS ENQUIRIES OUTSIDE STATED LIMITATIONS SHOULD BE REFERRED TO DOCUMENT EXCHANGE, PO BOX 1500, EDINBURGH, SA 5111, AUSTRALIA					
16. DELIBERATE ANNOUNCEMENT No Limitations					
17. CASUAL ANNOUNCEMENT Yes					
18. DEFTEST DESCRIPTORS Spatial distribution Surface clutter Target recognition Radarfrequency interference Parameter estimation					

19. ABSTRACT

The spatial distribution of surface clutter in general depends on radar resolution, grazing angle and scatterers on the surface. The Weibull, K- and lognormal distributions are commonly used to approximate the clutter spatial distribution. Comparisons among all three distributions are reviewed and extended. Statistical properties of the Weibull and K-distributions in the log domain are derived and then used in new approaches, named as unbiased estimation schemes, for faster parameter estimation for the Weibull and K- distributions. The maximum likelihood estimates for the K-distribution are also derived without the need of the derivative of the Bessel funtion. The proposed unbiased estimation schemes provide nearly as identical estimates as the maximum likelihood scheme does, according to real aperture radar data and synthetic aperture radar data analysed.

Page classification: UNCLASSIFIED